Czech Technical University in Prague

Faculty of Mechanical Engineering

Department of Automotive, Combustion Engine and Railway Engineering

Master's thesis

Exhaust emissions from in-use motorcycles

Author: Antonín Voldřich

Study program: Master of Automotive Engineering

Supervisors: prof. Michal Vojtíšek Ph.D.

Satrio Wicaksono, S.T., M.Eng., Ph.D.

PRAGUE 2021

MASTER'S THESIS ASSIGNMENT

I. Personal and study details

Student's name: **Voldřich Antonín** Personal ID number: **456162**

Faculty / Institute: **Faculty of Mechanical Engineering**

Department / Institute: **Department of Automotive, Combustion Engine and Railway Engineering**

Study program: **Master of Automotive Engineering**

Branch of study: **Advanced Powertrains**

II. Master's thesis details

Master's thesis title in English:

Exhaust emissions from in-use motorcycles

Master's thesis title in Czech:

Emise výfukových plynů používaných motocyklů

Guidelines:

While emissions from automobiles and heavy vehicles have been characterized extensively in the laboratory and on the road, motorcycle exhaust emissions, despite being potentially considerable, have received much less attention. The goal of the thesis is to characterize the emissions of regulated and basic unregulated pollutants from several in-use motorcycles. For each motorcycle, coast-down data are to be obtained on a suitable test track to determine the road losses, chassis dynamometer is to be set to mimic the aerodynamic drag, rolling resistance and other losses, and exhaust sampling system is to be installed to allow measurement of exhaust flow, concentrations of gaseous pollutants and key properties of particulate matter such as total particle number or particle size distribution. The emission measurement is to be validated for a reasonable range of representative conditions by carbon balance, reference measurement or other suitable method. The effects of operating conditions on emissions should be discussed.

Bibliography / sources:

Platt, S.M., et al. (2014): Two-stroke scooters are a dominant source of air pollution in many cities. Nature communications 5.1, 1-7. // Vojtisek-Lom, M., et al. (2019): A miniature Portable Emissions Measurement System (PEMS) for real-driving monitoring of motorcycles, Atmos. Meas. Tech. Discuss., https://doi.org/10.5194/amt-2019-387. // Giechaskiel, B., et al. (2019): Identification and quantification of uncertainty components in gaseous and particle emission measurements of a moped. Energies, 12(22), 4343.

Name and workplace of master's thesis supervisor:

prof. Michal Vojtíšek, Ph.D., Department of Automotive, Combustion Engine and Railway Engineering, FME

Name and workplace of second master's thesis supervisor or consultant:

Date of master's thesis assignment: **30.10.2020** Deadline for master's thesis submission: **06.01.2021**

Assignment valid until: _____

prof. Michal Vojtíšek, Ph.D. Supervisor's signature	doc. Ing. Oldřich Vítek, Ph.D. Head of department's signature	prof. Ing. Michael Valášek, DrSc. Dean's signature

© ČVUT v Praze, Design: ČVUT v Praze, VIC

III. Assignment receipt

The student acknowledges that the master's thesis is an individual work. The student must produce his thesis without the assistance of others, with the exception of provided consultations. Within the master's thesis, the author must state the names of consultants and include a list of references.

30.10.2020

Date of assignment receipt

Student's signature

© ČVUT v Praze, Design: ČVUT v Praze, VIC

Annotation

Author:	Bc. Antonín Voldřich
Title in English:	Exhaust emissions from in-use motorcycles
Title in Czech	Emise výfukových plynů používaných motocyklů
Academic year:	2020/2021
Major	Advanced Powertrains
Department	Department of Automotive, Combustion Engine and Railway Engineering, Faculty of Mechanical Engineering (CTU in Prague) Faculty of Mechanical and Aerospace Engineering (ITB)
Supervisors	prof. Michal Vojtíšek Ph.D. Satrio Wicaksono, S.T., M.Eng., Ph.D.
Abstract:	The goal of the thesis was to characterize the emissions of regulated and basic unregulated pollutants from two in-use motorcycles. For each motorcycle, coast-down data were obtained on a suitable test track to determine the road losses, a chassis dynamometer was set to mimic the aerodynamic drag, rolling resistance and other losses, and an exhaust sampling system was installed to allow measurement of exhaust flow, concentrations of gaseous pollutants and key properties of particulate matter such as total particle number or particle size distribution.
Keywords	Emissions, motorcycles, pollutants, emissions testing, chassis dynamometer, coast-down testing, L-category vehicles, Exhaust gas analysis
Number of pages	95
Number of figures	47
Number of tables	17

Declaration

I hereby declare that I have completed this thesis independently and that I have listed all the literature and publication used in accordance with the methodological guidelines about adhering to ethical principles in the preparation of the final thesis.

In Prague, 10th of January 2021

……

Signature

Acknowledgements

Firstly, I would like to thank my mentor and supervisor prof. Michal Vojtíšek, Ph.D. and employers of the Czech University of Life Sciences Prague for their time, guidance, support and help with the diploma thesis. A big thanks also belong to my family for their support during my studies.

Table of Content

List of Abbreviations

a	acceleration
A	rate of absorption
AFR	air/fuel ratio
CH_4	methane
CI	compression ignition
CO	carbon monoxide
CO_2	carbon dioxide
CVS	constant volume sampler
DOHC	double overhead camshaft
DPF	diesel particulate filter
EEPS	engine exhaust particle sizer
EU	European Union
F	force
FID	flame ionization detector
FTIR	Fourier transformation infrared analyser
GPS	global positioning system
H	hydrogen
h	Planck constant
H_2O	water
HC	hydrocarbons
HCHO	formaldehyde
Hz	hertz
ICE	internal combustion engine
km	kilometre
kW	kilowatt
N_2	nitrogen
NDIR	nondispersive infrared analyser
NEDC	New European Driving Cycle
Nm	nanometre
NO	nitric oxide
NO_2	nitrogen dioxide
NO_x	nitrogen oxides
NSRC	storage and reduction catalyst
O_2	oxygen
O_3	ozone
OH	hydroxyl
p	pressure
PC	personal computer
PEMS	the portable emissions measurement system
PM	particulate matter
PN	particle number
POA	primary organic aerosol formation
ppm	particles per million
RDE	real driving emissions
RPM	rounds per minute
SCR	selective catalytic reduction
SCS	sample conditioning system
SI	spark ignition
SOA	secondary organic aerosol formation
SOHC	single overhead camshaft
SPN	solid particle number
t	time
TWC	three-way catalyst
USA	United States of America
v	velocity
V	volume
ν	frequency
VOCs	volatile organic compounds
W	Watt
WLTC	Worldwide Harmonized Light Vehicles Test Cycle
WLTP	Worldwide harmonized Light-duty vehicles Test Procedure
WMTC	World Motorcycle Test Cycle
Λ	Wavelength
λ	Relative air/fuel ratio
ρ	density

Introduction and the goals of the thesis

Emissions from internal combustion engines are currently an extensively discussed problem worldwide. It is well known that road transport vehicles contribute to environmental pollution which leads to undesired climatic changes and which can be harmful to human health. Emissions limits stated by legislation are becoming stricter over time which forces the producers of vehicles to pay attention to this problem thoroughly. Thanks to modern exhaust aftertreatment technologies the amount of emissions production is sufficiently being reduced but it is becoming more challenging every year to meet these requirements.

Regarding the emissions regulation, passenger cars and heavy vehicles have received much more attention in the past in comparison to vehicles from L-category (motorcycles, mopeds, quads etc.) These vehicles still do not have to comply with such strict requirements as the rest of the road vehicles despite being potentially harmful to the environment and human health as well. Small engines from these vehicles were one of the last categories of internal combustion engines for which emissions standards have been established. Even though they produce hundreds of harmful pollutants, so far only hydrocarbons (HC), carbon monoxide (CO) and nitrogen oxides (NO_x) are being regulated. Recently established European standard Euro 5 from January 2020 which made the limits of these pollutants for L-category stricter, suggests that this topic is relevant, and will be discussed even more in the future [1].

The main goal of this thesis is to characterize the emissions of regulated and basic unregulated pollutants from two in-use motorcycles. Coast-down testing is to be conducted and the evaluated results used for the optimal settings of chassis dynamometer to mimic the road losses. An Experiment of emissions measurement is to be conducted for both vehicles in a laboratory environment. An Exhaust sampling system is to be installed and exhaust gas flow, concentrations of gaseous pollutants and key properties of PM are to be measured. The obtained data are to be analysed and discussed. The whole experiment is then to be validated by a reasonable range of representative conditions by carbon balance, reference measurement or another suitable method. The effects of operating conditions on the formation of pollutants and on emissions shall be discussed.

In the first part of this thesis, the theory of this problematics will be explained. General principles of the combustion process, emissions formation, aftertreatment technologies, legislative requirements and emissions measuring methods will be described in order to build sufficient theoretical basis for the experimental part of this thesis.

In the second part, conducted experiment of gaseous and particulate emissions measurement will be described. The methodology of this experiment and its technical procedure will be explained. The measured data will be evaluated, and the results will be discussed and compared with current emissions limits stated by the legislation in Europe. The tested vehicles will be also compared between each other and the influence of operating conditions will be discussed.

1 Combustion process of ICE

Before discussing emissions formation during the driving operation of motorcycles and the principles of its measurement, it is convenient, firstly, to explain fundamentals of combustion process of internal combustion engines (ICE) and the principles of pollutants formation of ICE in general. This general information applies for motorcycles as well as for most of the other road vehicles. Terms such as spark ignition, compression ignition, perfect combustion and air/fuel ratio will be described in order to understand the creation of undesired pollutants in the exhaust gas.

In the basic combustion process, fuel (typically a mixture of hydrocarbon) and oxidizer (air or oxygen) undergo a chemical process to be changed into the products. The aim of this process in ICE is to transform the chemical energy from the fuel into the mechanical work of the piston and afterwards, to change that work into rotational movement of the crankshaft while heat is being released [2].

1.1 SI and CI engines

There are various ways how to divide types of internal combustion engines, but with respect to the emission formation, the only major distinction of spark ignition engines (SI) and compression ignition engines (CI) will be explained [2].

- In SI engines, a sparkplug initiates the combustion that makes the mixture of air and fuel burn inside the chamber which forces the piston to move downwards. SI ignition engines usually run on gasoline (petrol) fuel.
- In the compression ignited engines (CI), only air is being compressed to very high pressure, and fuel (usually diesel fuel) is sprayed inside the combustion chamber at the right time. That makes the mixture to ignite by itself which causes the same piston motion as in SI engines.

In both cases, certain amounts of pollutants are being created and it is strongly influenced by air/fuel ratio which will be explained below. Motorcycle vehicles contain mainly SI engines.

1.2 Stoichiometric Combustion

When there is exactly the amount of air needed to burn all fuel inside the combustion chamber, we talk about stoichiometric combustion.

This is a special case of combustion in which all reactants are perfectly changed to products. Unfortunately, that is usually not the reality, and so undesired compounds are created in the process of combustion. If there is enough oxygen available during the stoichiometric combustion, a hydrocarbon fuel can be completely oxidized. The hydrogen from the fuel is converted to water H_2O and the carbon to carbon dioxide CO_2. Even though air contains a high amount of nitrogen, it is not much affected by the reaction when the products are at low temperatures. The composition equation of a general hydrocarbon fuel of average molecular composition C_aH_b, where *a* and *b* are proportional coefficients, is stated below [2] [3]:

$$C_aH_b + \left(a + \frac{b}{4}\right)(O_2 + 3.773N_2) = aCO_2 + \frac{b}{2}H_2O + 3.773\left(a + \frac{b}{4}\right)N_2$$

In this equation, there is just enough oxygen to convert all the fuel into completely oxidized products [2].

1.3 Air/fuel ratio

Air/fuel ratio (AFR) and relative air/fuel ratio (λ) are important parameters of the combustion process. They describe the composition of the air/fuel mixture which strongly influences the formation of the pollutants.,

AFR is the ratio between the mass of air (m_{air}), and the mass of fuel (m_{fuel}) that are used by the engine during its operation [2].

$$AFR = \frac{m_{air}}{m_{fuel}}$$

For the stoichiometric combustion of gasoline fuel, AFR is around the value of 14.7:1 and it is called stoichiometric AFR (AFR_{stoich}). That means that for burning 1 kg of gasoline fuel completely, we would need 14.7 kg of air. The combustion occurs also when AFR is not stoichiometric which will be explained further below.

Table 1 shows the stoichiometric air/fuel ratios for different fossil fuels [2] [4].

Table 1: AFR for different fuels [4]

Fuel	Chemical formula	AFR
Methanol	CH_3OH	6.47:1
Ethanol	C_2H_5OH	9:1
Butanol	C_4H_9OH	11.2:1
Diesel	$C_{12}H_{23}$	14.5:1
Gasoline	C_8H_{18}	14.7:1
Propane	C_3H_8	15.67:1
Methane	CH_4	17.19:1
Hydrogen	H_2	34.3:1

Relative air/fuel ratio (λ), also named air/fuel ratio equivalence factor, is defined as [4]:

$$\lambda = \frac{AFR_{actual}}{AFR_{stoich}}$$

Depending on the value of relative air/fuel ratio, the engine can work with lean, stoichiometric or rich air/fuel mixture.

Table 2: Types of air/fuel mixtures [4]

Lambda	Air/fuel mixture	Description
λ =1	Stoichiometric	Exactly the amount of air required for the complete combustion of fuel
λ < 1	Rich	Not enough air to burn the fuel completely
λ > 1	Lean	More oxygen than needed for complete combustion.

2 Exhaust gas emissions

Exhaust gas contains two types of compounds that are considered undesirable:

- greenhouse gases, such as carbon dioxide CO_2, methane (CH_4) and nitrous oxide (N_2O)
- compounds hazardous to the environment or human health (or both), such as nitrogen oxides (NOx), carbon monoxide (CO), particulate matter (PM) and various organic compounds.

These pollutants will be described further in chapters 2.1 and 2.2. Transport vehicles can contribute to pollutants formation in various ways, not only by the formation of exhaust gas. As an example, we can name emissions from brakes, clutch and tyres wear, road surface wear and road dust resuspension. Considering the topic of the thesis, only pollutants formed in the exhaust gas will be discussed further.

It is also important to say that urban air pollution is a problem worldwide, caused not only by transportation but also by different sources (industry, power generation, local heating, mobile machinery etc.), however transport vehicles definitely strongly contribute to it. Emissions formation from motorcycles works on the same principle as emissions formation from other road vehicles so this chapter describes this phenomenon in general. The composition and amount of harmful substances depend on many variables, such as type of the engine, its state and fuel composition. It is also strongly influenced by the combustion process itself, and its parameters, such as air/fuel ratio (λ), combustion temperature and combustion timing. Furthermore, the type and amount of each pollutant depend on the aftertreatment devices used, such as three-way catalyst (TWC) for stoichiometric SI engines or diesel oxidation catalyst (DOC), diesel particulate filter (DPF), or selective catalytic reduction (SCR) for CI engines [2] [5].

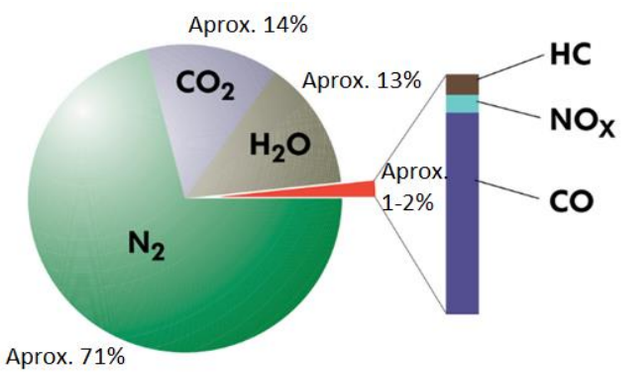

Figure 1: Exhaust gas composition in SI engines [6]

N_2 – Nitrogen

H_2O –Water

CO_2 – Carbon dioxide

O_2 – Atmospheric oxygen

CO – Carbon monoxide

NO_x – Nitrogen oxides

HC – Unburned hydrocarbons

PM-particulate matter

In Figure 1, we can see the basic composition of exhaust gas in SI engine during stoichiometric combustion. (Nitrogen and water are always present, and they are not considered pollutants) [6].

2.1 Health relevant pollutants

There are more than 1000 specific components of harmful substances formed during the combustion of ICE in SI and CI engines however the legislative limits only a few of them [2].

In case of incomplete combustion, the following substances can be observed as a part of exhaust gas: Carbon monoxide (CO), a mixture of volatile organic gases summed up as hydrocarbons (HC) and particulate matter (PM). These can be harmful to human health or our environment. If oxygen is used as an oxidiser, nitrogen represents the biggest portion of exhaust gas. Mainly due to high temperatures, compounds of nitrogen oxides (NOx) are being created. Those consist mostly of NO but also NO_2, usually in smaller amounts. Because of improper combustion, a certain amount of fuel and also a portion of the engine lubricating oil entering the combustion process do not get burned, causing a presence of unburned hydrocarbons in exhaust gas [2].

One of the most informative parameters for evaluating the composition of the combustion products is relative air/fuel ratio λ (see chapter 1.3) [7].

In the following graphs, regulated pollutants levels are displayed as a function of λ. It plays a huge role when talking about pollutants formation and the final composition of the combustion products [7].

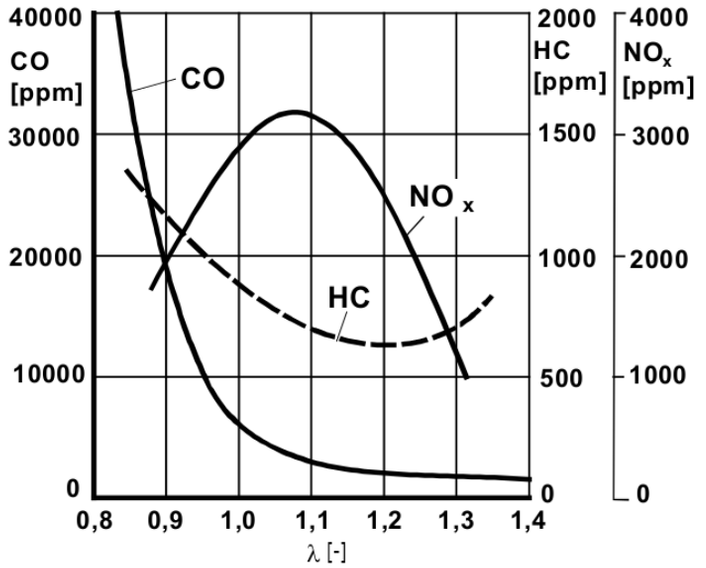

Figure 2 Pollutant emission levels as a function of relative air-fuel ratio (λ) for SI engines [7]

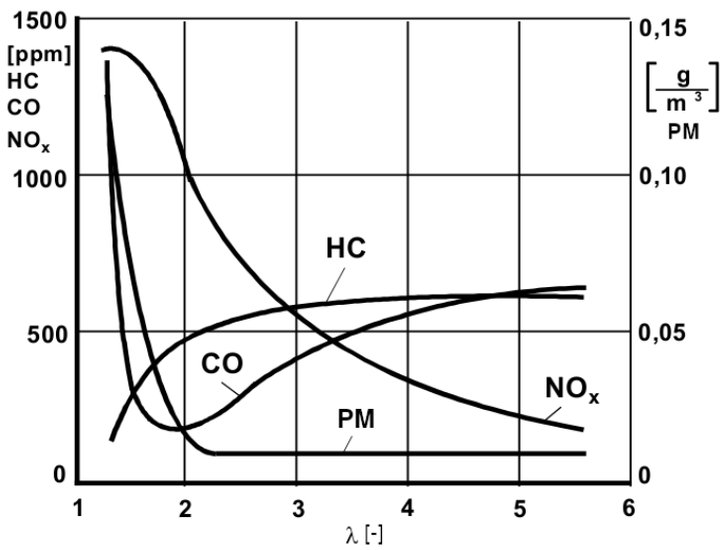

Figure 3: Pollutant emission levels as a function of relative air-fuel ratio (λ) for CI engines [7]

HC – unburned hydrocarbons

CO – carbon monoxide

NO_x – nitrogen oxides

PM – particulate matter (soot)

λ – specific air/fuel ratio

PPM – particles per million

g – gram

m^3 – cubic meter

From Figure 2 and Figure 3, it is evident that pollutants formation is different in SI and CI. The main difference is that CI engines usually work at leaner mixtures ($\lambda > 1$) and more PM is created. The following chapters will provide the most important information about the most relevant pollutants from the combustion process [2].

2.1.1 Carbon monoxide

Carbon monoxide (CO) is an intermediate product of combustion, the emissions of which are a sign of incomplete combustion. It has a negative effect on human health mainly because it reduces oxygen transport by haemoglobin. CO impairs the ability of the blood to bring O_2 to body organs and tissues and those can be therefore damaged. It can also cause health problems for people with cardiovascular diseases and in higher concentrations can be even poisonous [8] [9].

From Figure 2 it is obvious that most of CO is present in the richer mixture especially in SI engines. It is because there is not enough O_2 to transform CO into CO_2. In the near to stoichiometric air-fuel mixtures, due to high temperature, decomposition of CO_2 can cause another reason for CO formation. At very lean mixtures, small amount of CO is also created due to low temperature and slower chemistry, but it is not so significant. CO emissions in CI engines are low enough to be considered unimportant [2] [10].

2.1.2 Nitrogen oxides NOx

Under the common term NO_x, we describe a group of nitrogen oxides. The two most important of them are nitric oxide NO and nitrogen dioxide NO_2. Both are created during the combustion process of ICE, but NO in much higher scale, and both have a negative impact on global ecosystem and human health. They contribute to the phenomena of acid rains, global warming and creation of photochemical smog. NO_2 is more dangerous to human health than NO. It diffuses into the respiratory epithelium and dissolves there which can cause respiratory problems and airway inflammation. Even small concentrations are dangerous for humans especially in long exposures, and it can lead to development of asthma or other respiratory diseases [11] [12] [8].

NO is being created at high temperatures ($T > 1800K$) due to oxidation of atmospheric nitrogen N_2 (air consists of 78 % of N_2). As it can be seen in Figure 2, the maximum amount of NO is created at slightly lean air-fuel mixtures ($\lambda = 1.05–1.1$). The mechanism of NO

formation at near stoichiometric air-fuel mixtures has been described by Zeldovich and is referred to as the Zeldovich mechanism [2] [3] [10]:

$$O + N_2 = NO + N$$
$$N + O_2 = NO + O$$
$$N + OH = NO + H$$

NO_2 is very reactive substance which is formed from NO via reactions such as [2]:

$$NO + HO_2 \rightarrow NO_2 + OH$$

It is being decomposed back to NO in most cases, but if the flame is quenched by mixing with colder fluid, the following reaction does not happen [2].

$$NO_2 + O \rightarrow NO + O_2$$

Additional NO_2 is formed in oxidation catalysts used in many modern diesel engines which leads to NO_2 being tens of percent of NO_x. Due to this fact and also because of presence of flame quenching, NO_2/NO ratio is much higher in CI engines [2].

2.1.3 Hydrocarbons (HC)

Volatile organic gases summed up as hydrocarbons (HC) are being created as a product of incomplete combustion of the air-fuel mixture. They are especially dangerous for the human health because some of them have been proven to be carcinogenic [10].

Figure 2 and figure 3 show how specific air/fuel ratio influence the presence of HC. In the very rich mixture, there is not enough air to burn fuel properly, in very lean mixtures, due to low temperatures and hence slow chemistry some HC can be observed. In the near stoichiometric air-fuel mixture HC are present mainly because of [2] [8]:

- Local flame quenching
- Presence of crevices inside the combustion chamber
- Absorption of engine oil
- Sac volume on injector in CI

2.1.4 Particulate Matter

Under the term particulate matter (PM) we understand the sum of all solid and liquid particles suspended in air. It is a very complex mixture in which particles vary in size, composition and origin. Particles created during the process of combustion and mechanical processes such as friction are classified as primary particles while particles generated by chemical reactions in the atmosphere are called secondary particles. The smallest particles can have just a few nanometres while the biggest ones measure a few micrometres. A typical size distribution can be seen in Figure 4 [13]. Most of the particles, when talking about the number distribution, are smaller than 0.1 micrometres, unfortunately, those are also the most dangerous ones [2] [13] [14].

PM emitted from ICE is usually composed from solid carbon with absorbed hydrocarbons and sulfates. The particles are responsible for harmful effects on human health even in the absence of other pollutants. The most dangerous are the very small particles (ultrafine particles, nanoparticles) because they can get from the respiratory system and lungs directly to the blood. They can damage cardiovascular and lung system and contain carcinogens. PM also causes visible smog in urban areas [8] [10].

The amount of PM in exhaust gas of a vehicle can be defined by the particulate mass (PM), the total mass of particles and by the total particle number (PN), both being regulated as a part of Euro standards in Europe in passenger vehicles application [14]. However, PM production in general is so far still not regulated for SI vehicles from L-category.

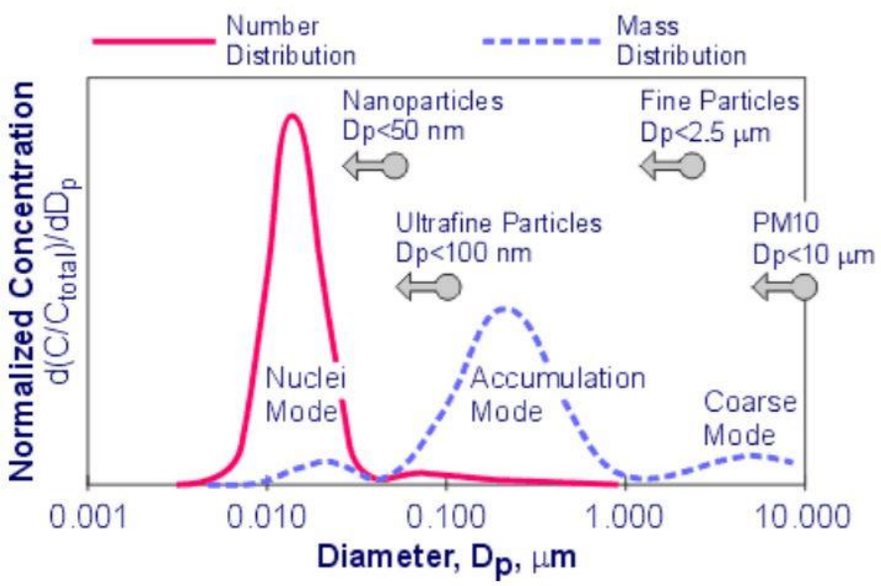

Figure 4: Size distribution of PM [13]

2.2 Greenhouse gases

Under the term greenhouse gases, we commonly understand gases that somehow participate in the greenhouse effect. This effect is basically a process of a gradual warming of the Earth surface. After the infrared radiation emitted from the Sun reaches the atmosphere, some of it is reflected back into space while the rest is absorbed and re-radiated by greenhouse gases. These gases radiate energy in all directions, and part of it is directed to the surface which causes its warming leading to the phenomenon of global warming [15].

The primary greenhouse gases that can be found in the Earth's atmosphere are water vapour (H_2O), carbon dioxide (CO_2), methane (CH_4), nitrous oxide (N_2O) and ozone (O_3).

During the complete combustion, carbon dioxide CO_2 is created. Even though it is created in every combustion process in ICE as the main product together with water, it is still considered a pollutant because it contributes to greenhouse effect [2].

During the combustion process of ICE, CH_4 can be emitted and also N_2O can be formed in aftertreatment devices, usually as a by-product of reactions of three-way catalyst (TWC), but so far without any regulations in Europe. In the experimental part of this thesis, the concentrations of these gases were measured together with other regulated and unregulated emissions [15].

2.3 Other unregulated emissions

While emissions of the regulated pollutants continue to decrease, thanks to emissions regulations such as Euro standards, unregulated emissions can be still present in large concentrations in exhaust gas of vehicles despite their potential harmfulness. Particles smaller than the size limit of the specific standard (currently 23 nm in Euro 5b and Euro 6) are not being regulated even though they can already be detected and can be dangerous to human health. For SI vehicles of L-category particles are still not regulated so far [16].

During the combustion process of ICE, other in light-duty vehicles unregulated harmful emissions are created, such as ammonia (NH_3) and toxic aldehyde formaldehyde (HCHO), both analysed during the experimental part of this thesis. They both proved to be harmful to human health. NH_3 is known toxic and dangerous for the environment and it also contributes to a secondary formation of particulate matter, while HCHO was proved to be carcinogenic. [16] [17].

2.4 Aftertreatment Systems

To reduce the undesired emissions from both, CI and SI engines, after they have been already created, several types of aftertreatment technologies are widely used. These technologies are the reason why current pollutants levels could be lowered according to legislative demands. The most common systems for this procedure are [18] [19]:

- Diesel particulate filter (DPF)
- Selective catalytic reduction catalyst (SCR)
- Diesel oxidation catalyst
- Three-way catalyst (TWC)
- NOx storage and reduction catalyst (NSR)
- Gasoline particulate filter (GPF)

Considering the topic of the thesis, only Three-way catalyst will be explained in detail because that is the most common system used in motorcycle operations.

2.4.1 Three-way Catalyst

The three-way catalyst (TWC) is an aftertreatment system which contains precious metals rhodium, platinum and palladium. Typically, it contains a ceramic monolith with parallel channels. A simplified scheme of TWC can be seen in Figure 5 [2] [20]:

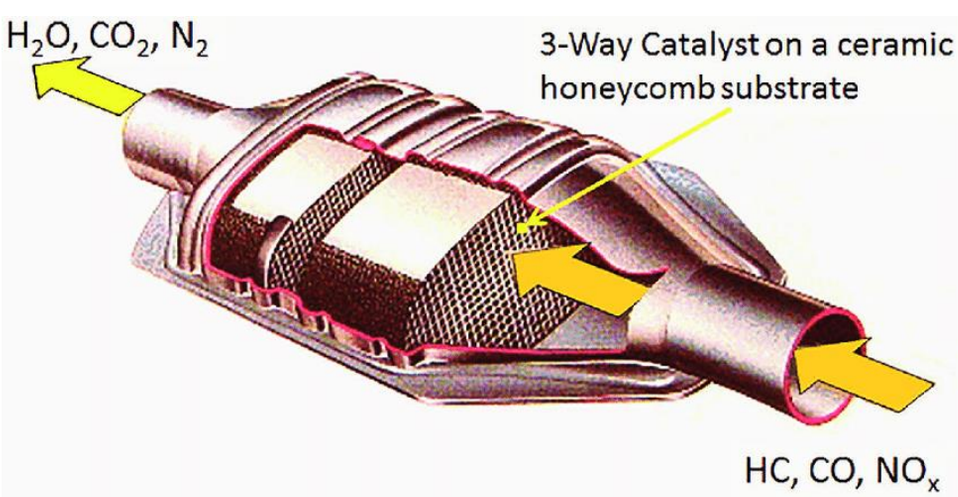

Figure 5: Scheme of the three-way catalytic converter] [21]

This type of catalyst is used mainly for SI engines that operate at the stoichiometric mixture. It can control the emissions of NOx, CO and HC but only when the air/fuel mixture is very close to 1 (λ ≈ 1). TWC works on the principle of oxidation of HC and CO, and reduction of NO as it can be seen in the following equations [2] [20].

$$CO + 0.5 \cdot O_2 = CO_2$$
$$HC + O_2 = CO2 + H_2O$$
$$CO + NO_x = CO_2 + N2$$

This can be sufficient only under the condition of precisely stoichiometric air/fuel mixture ((λ =1). If the mixture is far from stoichiometric the TWC is losing its efficiency as it can be seen in Figure 6. Therefore, λ must be measured and controlled constantly to stay as close to stoichiometric as possible [20]. Usually, one oxygen sensor (Lambda probe) is positioned before the catalyst and one after it, to measure the catalyst efficiency [22].

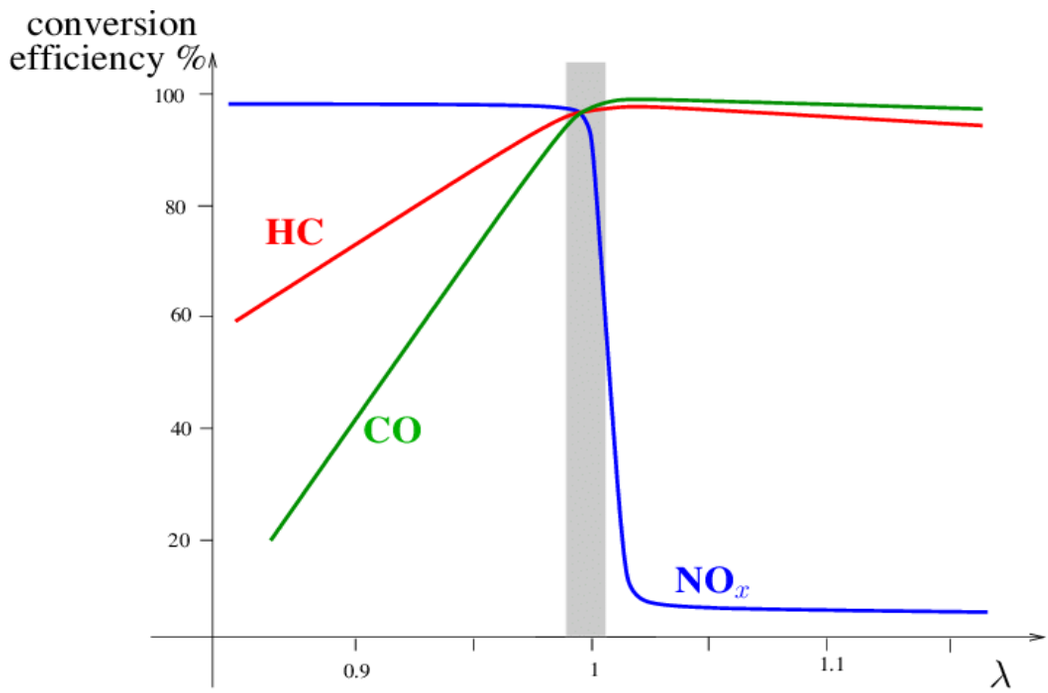

Figure 6: TWC efficiency [22]

2.4.2 Aftertreatment systems for motorcycles

Motorcycle vehicles make higher demands on engine accessories compactness and engine output than passenger cars. It can be difficult to control emissions formation while taking these two factors into account. The main steps towards cleaner exhaust gas in the past

have been the replacement of 2-stroke with 4-stroke engines and replacement of carburettors by fuel injection systems. The most common aftertreatment system for motorcycles today is compact TWC working on the same principle as explained in chapter 2.4.1. Compared to passenger vehicles, when this technology is used in motorcycles, only one oxygen sensor is present, and it is positioned before the catalyst. For the catalyst to work efficiently, air/fuel mixture must be precisely stoichiometric ($\lambda = 1$), the same as for passenger cars [23].

Also, often oxidation catalysts are used. When an engine combusts a rich mixture and high amounts of CO and HC are formed in the exhaust, additional air is mixed with the exhaust gas before the catalyst. This way the mixture becomes leaner and it is then possible to reduce CO and HC from the exhaust gas more efficiently.

3 Emissions legislation

Because of a potential emissions harmfulness and negative impact on the environment and society, emission standards were created. They were designed to regulate the amount of toxic exhaust gases, released into atmosphere from all types of vehicles and mobile machinery, also from a range of stationary sources, from household stoves to coal-fired power plants. The relevant emission standards depend on the geopolitical location and even though the trend is to unify them, they are still applied separately in each region (US, EU, China etc). Current development of powertrains used in road vehicles is strongly affected by the emission standards regulations and vehicle manufactures must adapt to it accordingly [24].

The first emissions standards regarding the automotive industry were introduced by the Clean Air Act, in the United States in 1963 as a reaction to the current pollution situation. Soon after that, similar standards were being created in other developed countries around the world [24] [25].

3.1 European emission standards

In the European Union and in the Europe Economic Area countries, so-called Euro emission standards are applied. These were firstly introduced in 1992 with Euro 1 and have been evolving since then. They define the acceptable limits for exhaust pollutants, such as CO, HC, NO_x, and PM from vehicles. The emissions of greenhouse gases are also regulated in Europe but not by Euro standards. Each Euro stage is stricter and more demanding than the previous one [1] [26].

All vehicles are divided into categories according to their type and each category has its specific emissions limits. Currently (2020), stage 6d is applied for passenger cars and it sets the relevant exhaust emissions limits for vehicles manufactured after January 2020. The development of Euro emissions standards for passenger cars running on gasoline fuel can be seen in Table 3.

Motorcycles fall in the vehicles of Category L (two- or three-wheel vehicles and quadricycles, such as quads and minicars). They can be further divided into several classes (1, 2–1, 2–2, 3–1 and 3–2) according to their maximal achievable speed and engine size. For each class, the emissions standards determine allowed emissions limits. Since 1st of January 2020, newly produced motorcycles must satisfy Euro 5 requirements [27].

The Euro 4 and recent Euro 5 limits for vehicles in L-category including motorcycles can be seen in Table 4. From a comparison with Table 3 is apparent, that the limits for L-

category vehicles are milder and currently the same requirements are applied for them, as they were applied for passenger cars between years 2009 and 2014. Particulate matter emissions for SI vehicles in L-category are so far still not regulated even though it is proved that they occur in non-negligible amounts (see chapter 5.3) [1] [26].

Table 3: Development of Euro limits for passenger vehicles with SI engines [23] [25]

Euro standard	Date	CO	Total HC	HC + NO_x	NO_x	PM	PN
	g/km						– /km
Euro 1	1992	2.72	–	0.97	–	–	–
Euro 2	1996	2.2	–	0.5	-	–	–
Euro 3	2000	2.3	0.20	–	0.15	–	–
Euro 4	2005	1	0.10	–	0.08	–	–
Euro 5	2009	1.0	0.10	–	0.06	0.0045	–
Euro 6	2014	1.0	0.10	–	0.06	0.0045	$6 \cdot 10^{11}$

Table 4: Euro 4 and Euro 5 limits for L-category vehicles with SI engines [28]

Euro standard	CO	Total HC	Non-methane HC	NO_x	PM	PN
	(g/km)					– /km
Euro 4	1,14	0,17	–	0,09	–	–
Euro 5	1,00	0,10	0,068	0,06	–	–

To evaluate if the vehicle meets the Euro standards requirements, there are the following types of testing according to the legislation. Considering the topic of the thesis, only the first type will be discussed in detail in the following chapters [1] [29].

- Tailpipe emissions
- CO emissions test at idling speed
- Crankcase gases emissions
- Evaporative emissions
- Durability of anti-pollution devices
- Low-temperature test
- Onboard diagnosis
- Real driving emissions – RDE (not yet for motorcycles)

3.2 Driving cycles

In order to simulate real driving conditions in a laboratory setup, emissions driving test cycles were created. They are commonly used for emissions and fuel consumption measurement of internal combustion engine vehicles. These cycles often consist of sub-cycles, each of which represents different driving conditions in different situations. A typical driving cycle is defined by vehicle speed and convenient gear change (if a manual transmission is present) as a function of time. It is also determined how much the actual speed in comparison to the prescribed speed can differ. In this chapter, NEDC, WLTC and finally WMTC cycle used for motorcycles will be described.

Selection of the right driving cycle for a specific vehicle measurement depends on the following factors [30] [31] :

- Type of vehicle
- Vehicle size according to the standardized categories
- Date of homologation
- Area of homologation

3.2.1 NEDC cycle

The shortcut NEDC stands for the New European Driving cycle. It was established in the 1980s to simulate firstly, urban but later also non-urban driving conditions of different types of road vehicles. For passenger cars testing, the whole test took 1180 seconds, with an average speed of 33.6km/h, maximal speed of 120km and the total distance of 11.03 km. It was created as a combination of two sub-cycles [32] [30] [33]:

- ECE- urban sub-cycle (low speed, low load, frequent stops)
- EUDC-extra-urban sub-cycle (high speed, high load, no stops.)

For passenger cars, the NEDC test consisted of 4x ECE and 1x EUDC sub-cycle as it can be seen in the following graph. For motorcycles the cycle looked exactly the same but there were 6x ECE sub-cycle instead of just 4 as for passenger cars while only one EUDC cycle remained unchanged [30] [31].

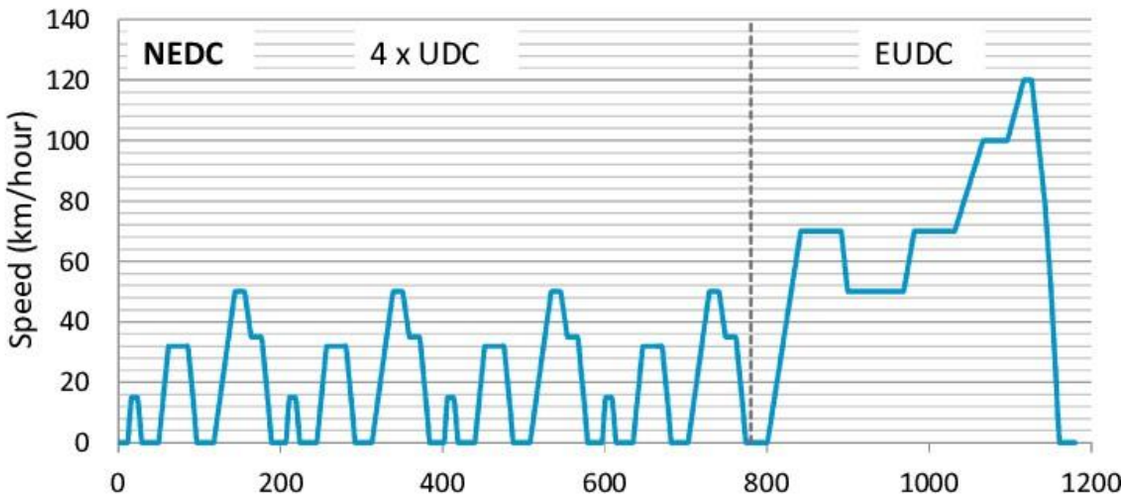

Figure 7: NEDC cycle for passenger vehicles (Euro 3) [31]

The NEDC test has been criticized that it does not replicate real-world driving conditions and the test itself was outdated, and so since 1 September 2019, it has been fully replaced with WLTC cycle [34].

3.2.2 WLTC cycle

The driving cycle WLTC (Worldwide Harmonized Light Vehicles Test Cycle) is currently the most relevant driving cycle in Europe. Together with RDE testing, they are part of WLTP (World Harmonised Light Vehicles Test Procedure). WLTC should realistically simulate current driving patterns in different environments. It consists of four phases [30] [35]:

- Low – urban traffic
- Medium – suburban traffic
- High – Rural traffic
- Extra-high – highway traffic

There are various modifications of the WLTC cycle and choosing the right one depends on the vehicle class. WLTP cycle is more dynamic than the previous NEDC, it simulates higher speeds and accelerations, and its results are more realistic than those in the previous driving cycles [30] [35].

In Table 5, we can see the comparison of the main parameters of the NEDC and WLTP cycles [30]:

Table 5: The comparison between NDEC and WLTC cycle [30]

Parameter	NEDC	WLTC
Duration (s)	1180	1800
Distance (km)	11.03	23.27
Average speed (km/h)	33.6	46.5
Maximum speed (km/h)	120.0	131.3
Stop duration (%)	23.7	12.6
Constant driving duration (%)	40.3	3.7
Acceleration duration (%)	20.9	43.8
Deceleration duration (%)	15.1	39.9

Unlike the NEDC cycle, the gear selection for the manual transmission must be defined for each vehicle separately to achieve the correct results. The example of the WLTC cycle for passenger cars can be seen in Figure 8 [30] [31].

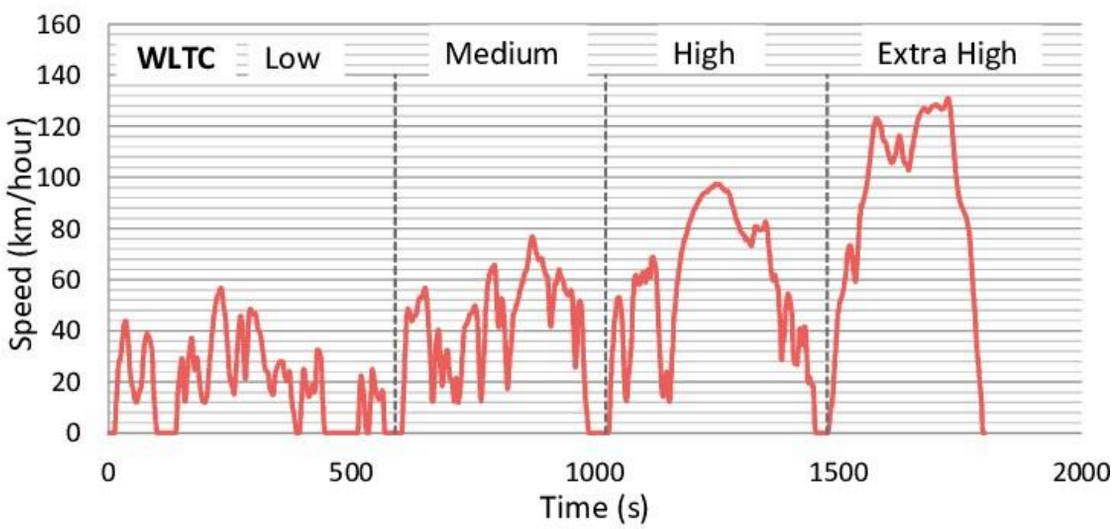

Figure 8: WLTC cycle for passenger vehicles [31]

3.2.3 WMTC cycle

The driving cycle WMTC (World Motorcycle Test Cycle) is an equivalent of WLTC but specially modified for the basic driving conditions of motorcycles. Similarly, to a normal WLTC cycle, it is divided into sub-cycles, but in this case, only in three (low, medium and high). For each motorcycle, for which the WMTC cycle is applied, the gear ratios must be calculated individually. This can be done either by a calculation according to the current

legislation or by using a predefined program in Microsoft Excel that calculates the desired ratios according to these input parameters [36] [37]:

- Vehicle mass
- Maximal RPM of the engine
- RPM in idling
- The ratio between RPM and speed for each gear ratio
- WMTC class according to the maximal speed of the vehicle
- Maximal power of the vehicle

The mentioned program for gear ratio calculation can be found at the following link [37]:

https://unece.org/worldwide-harmonized-motorcycle-emissions-certificationtest-procedure-wmtc-informal-group

The example of the WMTC cycle for the 3-2 class motorcycles can be seen in the following graph [38]:

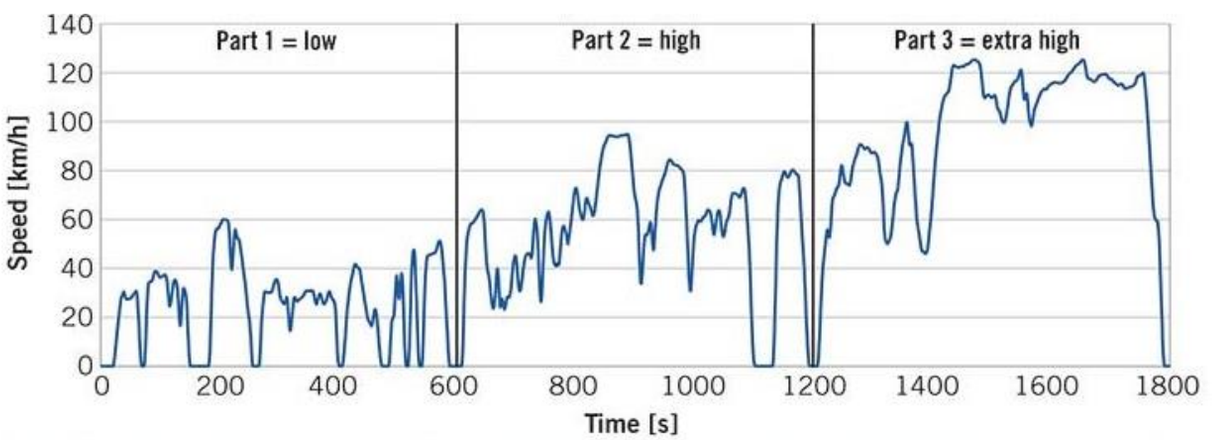

Figure 9: WMTC cycle for 3–2 class motorcycles [38]

4 Measurement of emissions

Measurement of emissions is being conducted for various reasons. It is necessary if we want to compare actual levels of pollutants with the limits required by the legislation. In this chapter, basic principles of emissions testing, exhaust gas sampling and specific emissions measuring methods will be explained. These principles apply not only for passenger vehicles but also for motorcycles and other road vehicles in general. Further information about motorcycles emissions measurement is then explained in chapter 5.

4.1 Emissions testing

During the life cycle of a vehicle, there are 3 basic phases of emissions testing according to the legislation:

- Homologation tests during the product approval (before actually starting the manufacturing of the vehicle.)
- Control tests for comparing newly manufactured product with quality requirements.
- Tests made during driving the vehicle (when it is already manufactured and available on the market) to ensure compliance over a variety of conditions and over the vehicle useful life.

(In addition, in regions with excessive air pollution, periodic inspections and maintenance programs are used to detect malfunctions in individual vehicles.)

The tests are typically done in an accredited testing laboratory where they undergo a required driving cycle, during which the concentrations of pollutants in exhaust gas is measured by special analysers [10] [39].

4.2 Exhaust gas sampling

Before emissions can be measured and evaluated, exhaust gas must be sampled from the exhaust system. Generally, we can divide laboratory emission measurement into 3 basic methods. The first method describes the situation where an exhaust gas sample is sent to emission analysers in the raw and undiluted form. In the second method, the sample is diluted with air before further analysis. In the last method, the sample is being collected without a presence of analysers during the driving of the vehicle, and it is examined later in a laboratory. In most cases, diluted sampling is being used. The dilution of the gas can be performed either in a partial flow dilution system or in a full flow dilution tunnel, such as the

CVS system which will be described further below. Choosing the right sampling method depends on specific emission analysis requirements and exhaust gas properties [10] [40].

4.2.1 Raw gas sampling

In the raw gas sampling method, the sample exhaust gas that is measured is not diluted with air. This method is commonly used for the relative simplicity of the sampling system, but it can be difficult to obtain reproducible and reliable results because of the high concentration of moisture, particulates, and high temperatures. Most of the measuring instruments are designed to operate close to ambient temperature and therefore cannot be used for raw gas sampling. Only instruments that can handle the high concentrations of raw exhaust constituents and high working temperatures can be used, those are for example smoke meters and opacity meters [10] [40] [41].

To obtain the total mass of measured emissions, it is crucial to measure gas flow simultaneously. In Figure 10, we can see a scheme of the raw gas sampling method. Part of exhaust gases is removed and filtered. The sampled gas is often conditioned by dehumidifier (cooler) until it becomes a dry sample which decreases its volume but also increases the concentration of each constituent. In special cases, the sample is not being dehumidified but humidity is preserved [10] [40].

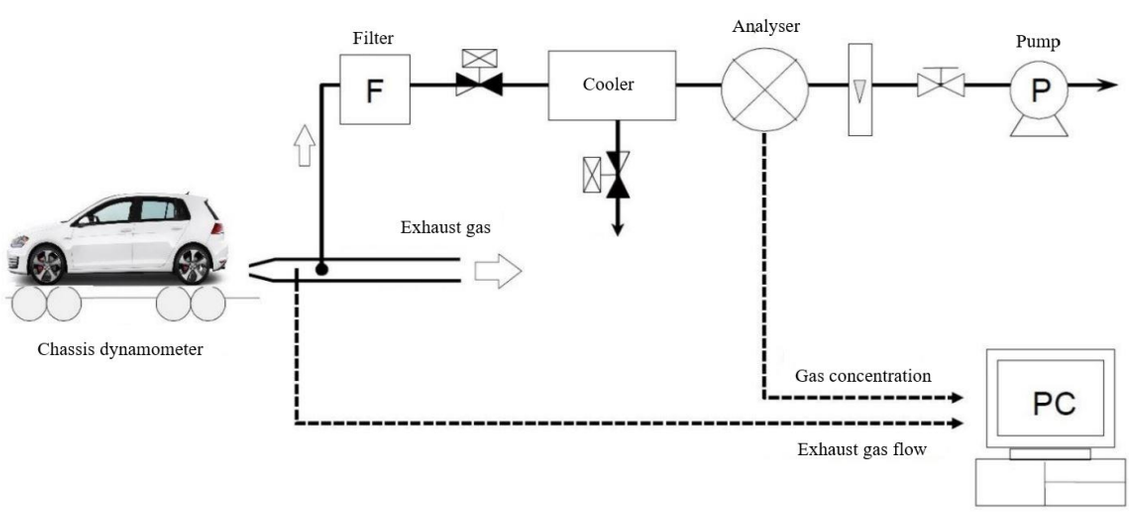

Figure 10: Scheme of raw sampling method [41]

4.2.2 Diluted sampling

The diluted sampling method is based on the principle of diluting exhaust gas sample with air. Because most of the measuring instruments cannot be operated in temperatures

much higher than ambient temperature, a gas sample is being cooled down to a required temperature level while avoiding or at least minimizing condensation and other chemical changes of the measured species. The concentration of water in the sample is being reduced to prevent condensation in the sampling train [40].

The most common method of diluted gas sampling is a Constant Volume Sampler (CVS). It is a system based on diluting a gas sample flow with the ambient air while preserving constant flow of the diluted gas. It is used in case of measuring total mass and it can especially useful when a sample has high concentrations or there is small exhaust gas flow [40] [41].

In Figure 11, we can see a simplified scheme of the CVS method. A sample is diluted with ambient air with preservation of constant volumetric flow. For the volumetric flow to remain constant, exhaust gas is being diluted with different amount of air according to actual exhaust gas flow. The total flow of the diluted exhaust gas is maintained by a pump. At the place, with a constant volumetric flow, the diluted exhaust gas is extracted and sampled into bags and/or analysed online. After finishing the procedure, individual components in the sampling bag are being analysed and mass of each compound is calculated from their concentrations, density and the total flow in CVS [40] [41].

Because the ambient air that is used to dilute the sample can also contain emissions

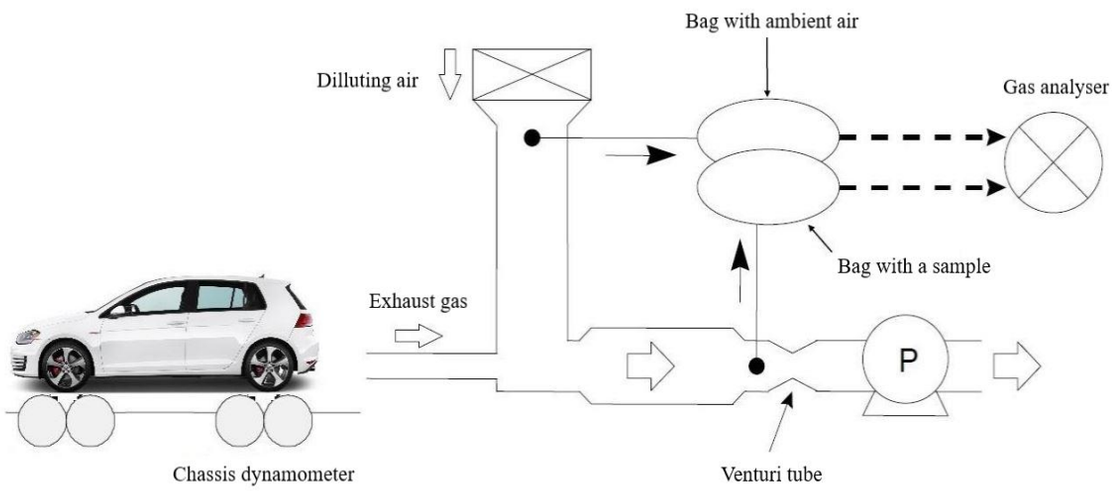

Figure 11: Scheme of CVS [41]

compounds, separated sampling bag is used to collect the ambient air. Concentrations of compounds in ambient air are analysed and subtracted from those in the diluted sample. The results are used for correcting the calculation of final concentrations in the sampling bag [40] [41].

4.3 Chassis dynamometer

A chassis dynamometer is a device used for vehicle testing which simulates real driving conditions in a controlled environment. For that, a roller assembly connected to a dynamometer is used as it can be seen In Figure 12. The resistance is simulated according to the driving resistances from real driving conditions. The tested vehicle is placed onto the rollers and must be well secured against sliding off. The convenient measuring devices sample part of exhaust gas and the rest exits the testing building via outgoing exhaust system [42].

Figure 12 Chassis dynamometer [author]

There are many types of chassis dynamometers according to a vehicle type (motorcycles, cars, trucks, tractors etc). The main applications for chassis dynamometers are [42]:

- Power and torque measurement
- Noise measurement
- Emission measurement
- Electromagnetic testing

The construction of chassis dynamometer can differ, but most often one big roller is used. There are three basic modes of chassis dynamometer measurement [42]:

- Keeping a constant tractive force – dynamometer is still making the same amount of resistance no matter the speed.
- Keeping a constant speed – dynamometer is controlling the tractive force made by a tested vehicle with speed remaining constant.
- Road load simulation – resistance is changing dynamically as a second-degree polynomial function of road losses with respect to speed. The road load coefficients (F_0, F_1, F_2) are different for each vehicle.

4.4 Measurement of exhaust gas flow

For the raw gas sampling method, it is necessary to know exhaust gas flow in order to calculate the mass of emissions. There are many ways how to measure gas flow directly such as flow measurement using pitot tubes, ultrasonic flow meters, volumetric flow meters etc. Exhaust flow can be also measured indirectly by calculation from intake air flow or fuel consumption. Considering the chosen experimental approach of this thesis, only direct flow measuring with the pitot-static tube will be explained in detail.

It is important to state, that flow measurement can be problematic because the conditions of exhaust gas such as temperature, pressure, composition, or flow speed are very unstable and change quickly in time. In smaller gasoline engines, there is also a risk of pulsation of the flow during idling which can influence the results, and even cause the opposite direction of the flow and dilution of exhaust gases with outside air. The flowmeter should be designed in such a way that these conditions do not influence the measured data. It is also important that the connected measuring device, due to changing the pressure drop or exhaust flow patterns does not influence the engine performance and the emission formation. Therefore, it is crucial to choose the right method, and make sure the measurement is not negatively influenced by any means [10] [41].

4.4.1 Pitot-static tube

A pitot-static tube (further only as pitot tube) also called Prandtl tube is an instrument used to measure flow speed. It is widely used in flow measurement applications in the automotive and aircraft industry. It can be used to measure air flow in pipes, ducts and stacks, and liquid flow in pipes, open channels, and weirs. The measuring principle is based on Bernoulli's principle where the increase of fluid speed causes decreases in its static pressure. By inserting the pitot tube directly inside the flow stream, static and total (stagnation)

pressure can be measured. From the pressure difference and the knowledge of the local temperature, the flow velocity can be calculated using the equation [43]:

$$v = \sqrt{\frac{2(p_t - p_s)}{\rho}}$$

v – flow velocity

p_t – total (stagnation) pressure

p_s – static pressure

ρ – flow density

This flow velocity is not an average velocity but actual velocity in the specific area of measurement. Pitot tubes can be used for both turbulent and non-turbulent flow, and they can be very small compared to the size of the pipeline where measuring takes place. They are especially useful for high flow or high-temperature applications. To receive accurate results, the pitot tube must be pointed directly into the air stream in a parallel way and the pressure sensors must have a sufficient measuring range. In Figure 13, there is a simple scheme of how the pitot-static tube functions [43] [44].

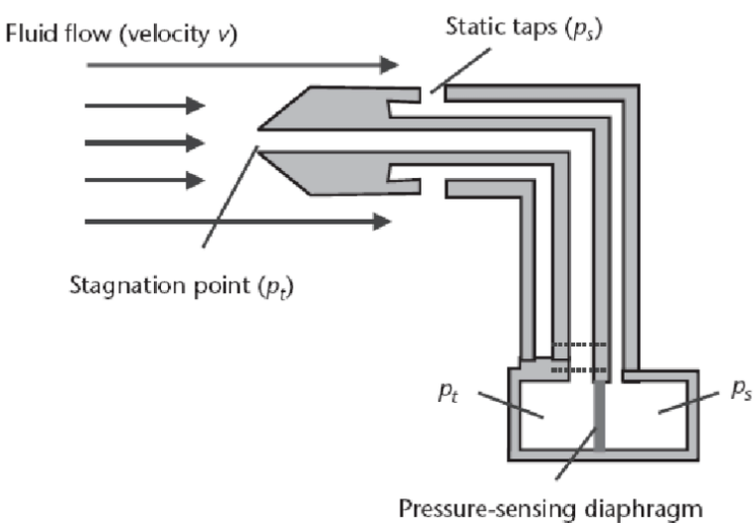

Figure 13 Pitot-static tube scheme [44]

4.5 Specific emissions measuring methods

There are several methods, how specific pollutants can be measured, and for that several types of analysers are used. Each analyser is able to measure different substances and works on a different principle. In the following chapters, the main principles of measuring gaseous emissions will be explained. For relevant results, it is important to use the convenient analyser with a sufficient range according to the character of a particular measurement.

Before measuring, the analyser must be also properly calibrated in order to ensure its correct functionality. For this procedure, often calibration gases are used [10].

4.5.1 Non-dispersive infrared analyser

Non-dispersive infrared analysers (NDIR) are used mainly to measure concentrations of CO and CO_2 emissions in exhaust gas. They can be also applied to the measurement of different gaseous emissions, but the procedure is more problematic.

The main principle is based on the fact that different gases absorb infrared radiation at specific wavelengths that, characteristic to their structure. In Figure 14 we can see absorption spectrums of CO, CO_2 and CH_4 [10].

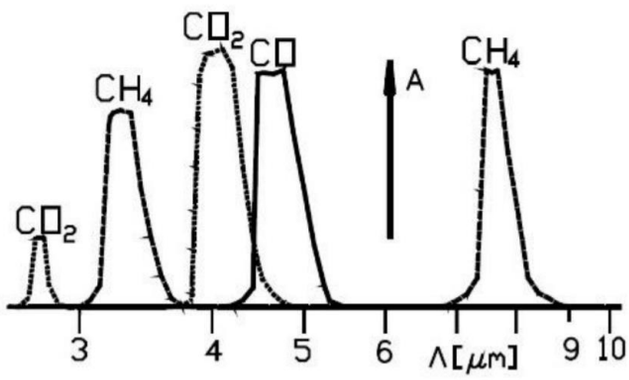

Figure 14: Absorption spectrum of CO, CO_2 and CH_4 [10]

Λ – Wavelength

A – rate of absorption

Infrared light source continuously sends infrared waves, usually through two identical tubes, one of them containing the exhaust sample, the other reference non-absorbing gas such as nitrogen. The detector then measures the intensity of wavelengths from both tubes and by comparing them, we receive a concentration of desired gas. For the specific wavelength selection, the filter wheel (Chopper wheel) is used. The simplified scheme of NDIR can be seen in Figure 15 [10] [45].

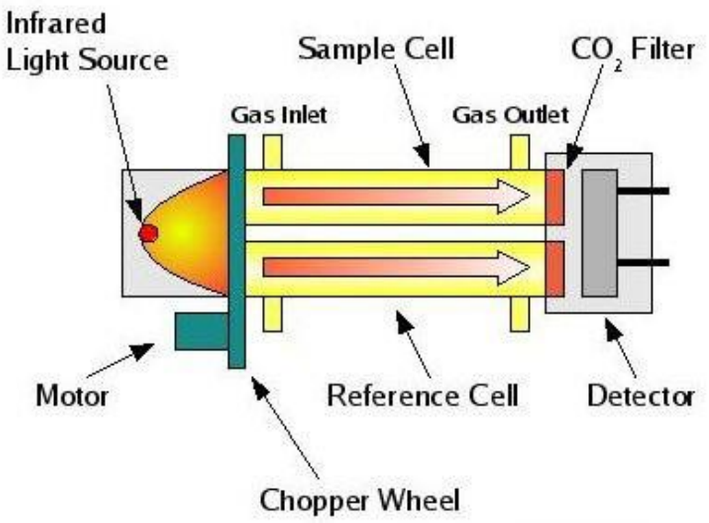

Figure 15 NDIR scheme [45]

4.5.2 Fourier transformation infrared spectroscopy

Fourier transformation infrared spectroscopy (FTIR) is based on the same principle as NDIR, it also works with the interaction between matter and infrared radiation, and measures concentrations of each substance. The main difference is that in FTIR it is possible to examine all wavelengths simultaneously while in NDIR only one at a time. FTIR measurement is also more precise and often faster than NDIR [46].

Every FTIR contains an interferometer working on the same principle as the Michelson interferometer. The schema of the FTIR interferometer can be seen in Figure 16 [46].

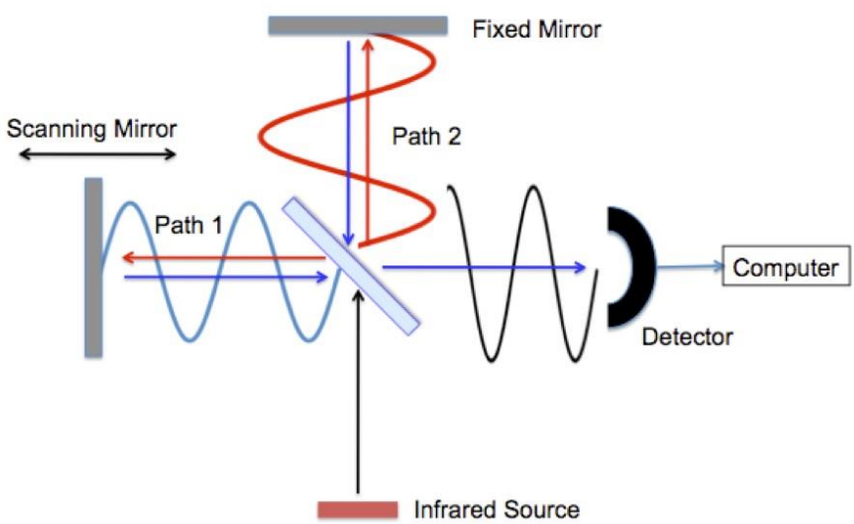

Figure 16:Scheme of FTIR interferometer [46]

The source generates infrared light which passes a sample through an interferometer which splits the light into two different parts: half of the light goes through the beam splitter while the other half is reflected. After that, the light beams from both paths recombine causing interference, pass through the sample, and reach the detector. The signal in the form of the interferogram is then transformed by using Fourier transformation into a single beam spectrum. Firstly, the background spectrum has to be collected without the sample present. Absorption spectra are then calculated, at each point, as a negative decadic logarithm of the ratio of sample to background spectra. The absorption spectra are then deconvoluted into absorption spectra of each relevant compound, and the concentrations of relevant compounds are calculated[46] [47].

4.5.3 Chemiluminescence analyser

Chemiluminescence analysers are used for measuring concentrations of NOx emissions in a gas sample. They work on the principle of measuring the amount of emitted chemiluminescent light during chemical reaction [10]:

$$NO + O_3 \longrightarrow NO_2 + O_2 + h.v$$

h – Planck constant

v – frequency

The intensity of this chemiluminescent light is directly proportional to the concentration of NO in the gas sample, and it is measured by a photodetector. For evaluating NO_2 concentrations, firstly NO_2 must be converted to NO, then the emitted chemiluminescent light is measured, and from that NO_2 concentrations can be calculated as the difference of the concentrations of NOx ($NO+NO_2$) and NO. It is necessary to supply oxygen into the analyser in order to create ozone required for the chemical reaction. This ozone is created in the ozone-generator which is part of the analyser [10] [48].

4.5.4 Flame ionization detector

Flame ionization detectors (FID) are mainly used for the measurement of hydrocarbons in a gas sample. In the hydrogen flame, hydrocarbons produce ions that can be detected. For that, a collector plate is used. When ions hit the plate, they induce a current that can be measured. The current is proportional to the ions production which is proportional to actual HC concentration present in the sample. To create a hydrogen flame, hydrogen and air

must be supplied in the right proportions in order to achieve reasonable results. A simplified scheme of FID can be seen in Figure 17 [10] [49] [50]:

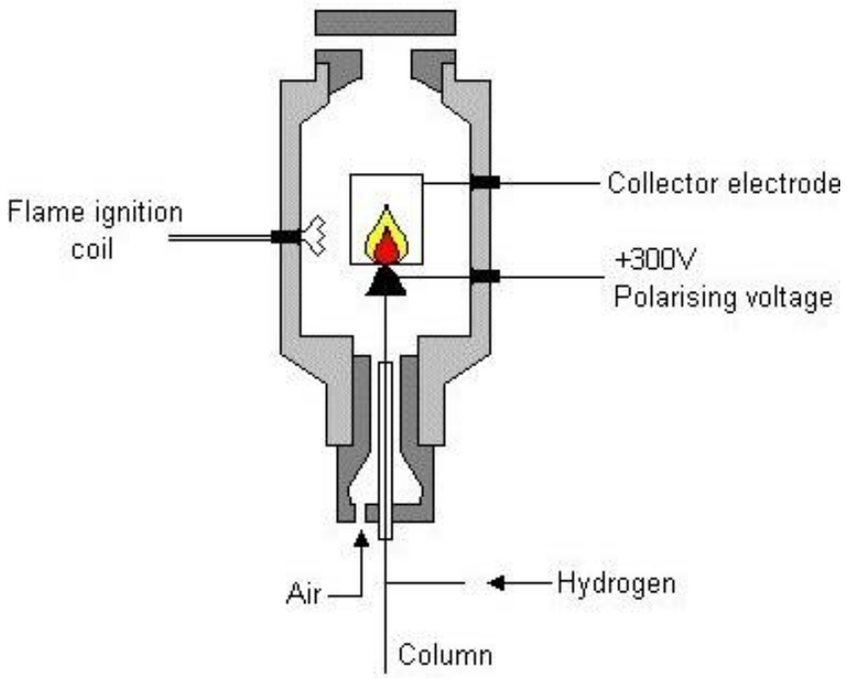

Figure 17: Scheme of FID [50]

4.5.5 Paramagnetic oxygen detector

Paramagnetic detectors use a unique physical property of O_2 which is its paramagnetic susceptibility. Unlike most of the other gases, when O_2 is nearby a magnetic field, it starts being attracted to it. The paramagnetic sensor contains a measuring cell with two glass spheres filled with nitrogen and mounted on a rotating suspension. Inside the measuring cell, a magnetic field is created by an electromagnet or permanent magnet, and it starts to attract the molecules of oxygen. That results in a force on the spheres which creates torque, acting on a suspension. This torque can be measured, and it is proportional to the oxygen content in the gas sample. The scheme of paramagnetic O_2 detector can be seen in Figure 18 [10] [51].

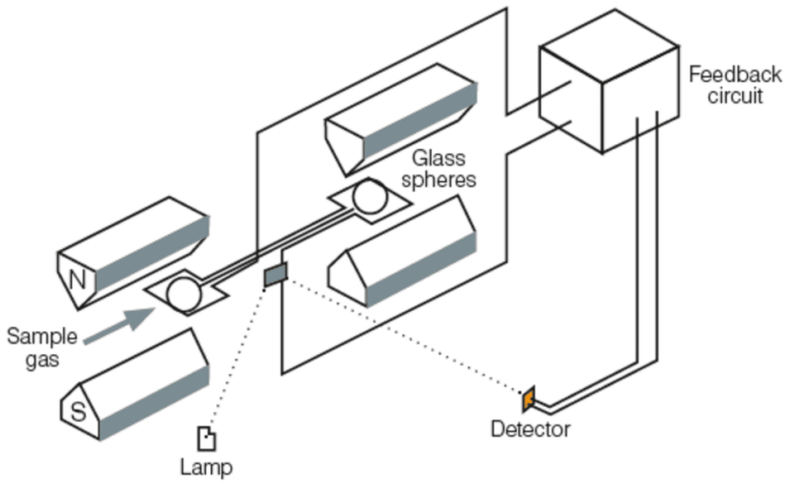

Figure 18 Paramagnetic O2 sensor [52]

4.5.6 PM measurement

The most important characteristics of PM in exhaust gas are particle mass and particle size. There are several instruments for measuring these characteristics, but only the most relevant according to the experimental part of this thesis will be explained [10] [53].

One of the approaches of particle mass measurement is the gravimetric method. It is based on weighing a gravimetric filter before and after sampling of a diluted exhaust gas [10].

The Engine Exhaust Particle Sizer (EEPS) is an instrument used for measuring PM size based on the principle of electrical mobility. Particles that enter the instrument are charged to a predictable level based on their size, pass through an annular space, and are repelled outward by the central column voltage to measuring electrodes located on the outside of the annular space. When the particles reach the electrodes inside the instrument, they release their charge, creating a very small current which can be measured by electrometers. This measured current is then converted into PM size distribution [54].

There are various types of particle counters based on different measurement principles. They are used for evaluating the particle number (PN). Currently, PN of non-volatile particles smaller than 23nm is determined according to the UNECE PMP legislative requirements. An example of such a device, which can differentiate volatile and non-volatile particles is NanoMet3, used in the experimental part of this thesis. It can determine the number of non-volatile particles bigger than 23nm by removing volatile particles by heated dilution. [55].

4.6 Real Driving Emissions testing

To ensure that vehicles follow the emissions limits not only in the laboratory environment but also during real driving conditions, Real Driving Emissions testing (RDE) was introduced for cars in the EU legislation. Since September 2017, RDE testing is now a

mandatory part of the WLTP procedure according to EURO 6 standard (for the time being only for passenger vehicles). The main difference between laboratory testing and RDE is the repeatability of the measurement.

While in the laboratory conditions, the same driving cycles can be driven repeatedly without too much of a difference, in RDE that is not possible. There are many factors that influence RDE testing such as unstable ambient conditions, traffic situation, driver behaviour and driving patterns, and each test has a different speed profile. Therefore, statistical methods must be used in order to evaluate data from the testing [1] [56].

The test itself consists of urban, rural and highway part, each of which lasts required time proportion of the total test. There are many other requirements regarding a valid RDE test, such as test duration, ambient temperature, elevation, vehicle speed, driven distance etc [56].

4.6.1 Portable Emissions Measuring System (PEMS)

For RDE testing, it is necessary to equip the vehicle with a measuring instrument that can be carried inside or moved with a vehicle during the whole testing. For that, Portable Emissions Measuring System (PEMS) is used. It is a device which measures concentrations of gaseous pollutants and particle emissions during RDE testing. There are several methods of how PEMS can be attached to a vehicle but the most common one is connecting it to a towing device of a vehicle. Heat resistant tube is connected to an exhaust system, and it brings the gas into flowmeter. The flowmeter is usually realised by a Pitot tube, and it measures the flow of exhaust gas. A sample of exhaust gas is then collected and transported into Sample Conditioning System (SCS) where it is adjusted, and finally, analysers are used for evaluation of emissions concentrations [58] [59].

Figure 19: PEMS installed on a passenger vehicle [57]

5 Measurement of emissions in motorcycles

Because most motorcycles use gasoline internal combustion engines, they participate in air pollution in a similar way as four-wheel vehicles. The principle of formation of these pollutants is the same as explained in chapter 2. The main harmful pollutants that are being formed in exhaust gas of motorcycles and that are regulated by the legislation are hydrocarbons (HC), oxides of nitrogen (NO_x) and oxides of carbon (CO, CO_2). There are also various pollutants that are not regulated including particulate matter. The measurement of emissions in motorcycles works on the same principles as explained in chapter 4. Tailpipes emissions measurement from motorcycles including coast-down testing and experiments conducted on this topic are described in this chapter.

Since 1st of January 2020, newly produced motorcycles must satisfy Euro 5 requirements (see chapter 3.1) The specific emissions measuring methods applied for motorcycles are the same as those for passenger vehicles (explained in chapter 4.5). The sampling methodology is also similar to the one used for passenger cars (see chapter 4.2) but usually specially designed CVS for motorcycles is used in order to obtain a diluted sample. Due to the topic of this thesis, only the first type of emissions testing will be described in detail in the following chapters [27].

5.1 Type I testing

The type I of emissions testing describes tailpipe emissions after a cold start. The testing is done on a chassis dynamometer in a laboratory environment, and WMTC cycle is used to simulate driving conditions stated by the legislation. The main requirements for type I testing are [27]:

- The testing room shall have a temperature of 298,2 ± 5 K (25 ± 5 °C).
- The vehicle shall be in a good mechanical condition and should be driven at least 1000 km before the test.
- The tyre pressure shall be adjusted to the specifications of the manufacturer.
- Appropriate reference fuel with density measured at 288,2 K (15°C) shall be used.
- The test driver shall have a mass of 75 kg ± 5 kg.

The vehicle speed tolerances in all time periods during the WMTC cycle are defined by upper and lower limits. The lower limit is 3,2 km/h lower than the lowest point on the

trace within one second of the given time, and similarly, the higher limit is 3,2 km/h higher than the highest point. Speed variations greater than these tolerances are acceptable if they occur for less than two seconds (for example during gear changes) [27].

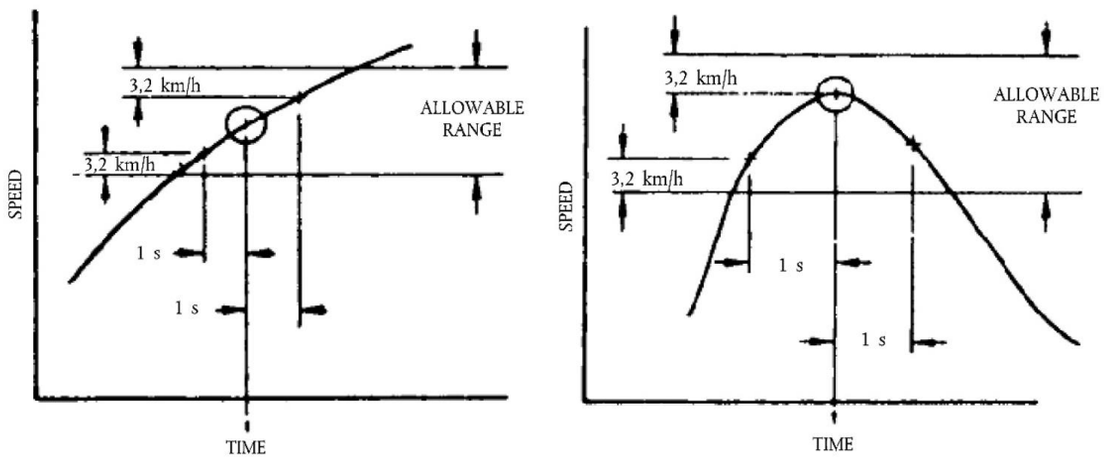

Figure 20: Range of acceptable vehicle speed tolerances [27]

5.1.1 Test I procedure

The test consists of prescribed procedures, such as dynamometer preparation and vehicle fuelling, conditioning and operating conditions. The goal of Test I is to evaluate the amount of CO, NO, and HC emissions, and to measure fuel consumption [27].

Before the test itself, dynamometer must be warmed up, and appropriately set for the measurement. The measured vehicle should be parked at the soak-area for between 6 and 36 hours prior to the test. After that, the drive wheel of vehicle should be placed on chassis dynamometer without starting the engine, cooling fan and sampling system shall be activated, and emptied sample collection bags (if present) should be connected. Then, sample flow rates and the gas flow measuring devices should be adjusted. After starting the flow measuring device, the vehicle is ready to start cranking. After that, transmission shall be put in gear, and the vehicle starts to accelerate according to the driving cycle. Two seconds after the end of the last part of the test, the engine should be turned off followed by the cooling fan and sampling system [27].

5.2 Coast-down testing

In order to derive a resistance force for chassis dynamometer settings, and thus to simulate real driving conditions in the laboratory environment, the so-called coast-down test is carried down. This road test consists of vehicle launch from a certain speed with the engine ungeared until the vehicle stops due to resistant forces. During this process, the vehicle speed and travelled distance are being recorded simultaneously. The main goal of coast-down testing is to evaluate the values of the road load forces, acting on the vehicle at certain road conditions and a certain speed. The sum of the road load forces consists mainly of aerodynamic drag roughly proportional to the second power of the speed, rolling resistance and grade resistance. These values are then used for the chassis dynameter settings before starting the required driving cycle. The measuring itself often takes place only in a specific speed range, such as from 120 km/h to 20 km/h [27] [60].

During the coast-down test, the vehicle steering shall be altered as little as possible so that its trajectory remains straight. Also, the brakes shall not be used until the end of the coast-down measurement period [27].

The coast-down time Δt_i corresponding to the specified speed v_j is the time required for the vehicle to decelerate from v_2 to v_1, while [27]:

$$v_1 = v_j - \Delta v$$
$$v_2 = v_j + \Delta v$$

Δv is determined according to the maximal speed of a vehicle. The same procedure is repeated in the opposite direction to measure the second coast-down time Δt_{bi}. The average Δt_i of the two measured cost down times Δt_{ai} and Δt_{bi} can be calculated using the following equation [27]:

$$\Delta t_i = \frac{\Delta t_{ai} + \Delta t_{bi}}{2}$$

This cost-down test should be done at least four times, and after that, average coast-down time can be calculated using the following equation [27]:

$$\Delta t = \frac{1}{n} \cdot \sum_{i=1}^{n} \Delta t_i$$

The result of coast-down testing is a curve representing speed as a function of road load forces. By polynomial regression, the equation of this curve can be obtained and can be used directly for the real road losses simulation in some types of chassis dynamometers. The general form of the target running resistant force *F(v)* as a function of speed can be seen below. Coefficients *a*, *b* and *c* are determined by the polynomial regression method.

$$F(v) = av^2 + bv + c$$

Chassis dynamometers with f_0 and f_2 coefficient digital setter use the following equation of the target running resistant force. The coefficients f_0 and f_2 are in this case directly input digitally:

$$F(v) = f_0 + f_2 v^2$$

It is also necessary to perform a coast-down test on a chassis dynamometer without any additional resistant forces. Then, the result coast-down curve is to be compared with the corresponding curve from the road coast-down measurement. Based on this comparison, the final dynamometer settings, which represent road load forces, are determined.

The tests must be done under the statistical accuracy smaller than 3% and should be repeated until this condition is satisfied. For the repeated tests it is important that the measurement conditions (warm-up procedure and coast–down starting speed) remain the same [27].

5.2.1 Coast-down test requirements

For the driver´s safety and the relevance of the results, legislation presents several requirements for the coast-down test that should be satisfied [27]:

- The driver shall sit on a vehicle in the standard position, and he shall wear well-fitting clothes and convenient protection.
- The driver shall have a mass of 75 kg ± 5 kg and be 1,75 m ± 0,05 m tall.
- The test road must be flat, level, straight and smoothly paved. The slope of the surface shall not exceed 0,5 % between any two points at least 2 m apart.
- The wind should be stable and should not exceed the average speed of 3 m/s.

- The ambient air temperature should be between 278,2K and 308,2K
- Relative humidity should not exceed 95%.
- When installing measuring instruments on the test vehicle, distribution of the load across the wheels and aerodynamic conditions should not be changed.

5.3 Topic related experiments

There has not been extensive research regarding the topic of emissions measurement in motorcycles, and it remains quite unexplored area in the automotive field. However, there has been some scientific work done by several authors, which will be discussed in this chapter.

M. Vojtíšek et al. with cooperation of the Technical University of Liberec designed emissions measurement device Mini-PEMS, a smaller version of PEMS which can be used for 2-wheel vehicles applications. Thanks to its compact size
(45 x 30 x 20 cm) and weight (≈ 15 kg), it can be mounted on a motorcycle or moped, and perform RDE measurements. It measures exhaust gas concentrations of CO, HC, CO_2, NO_x and O_2, together with engine speed, the inlet and exhaust gas temperature, the manifold absolute pressure, the geo-localization and vehicle speed. The exhaust mass flow rate can be then calculated from the engine emission and engine data. It proved to be an efficient tool for RDE testing with quite a reasonable accuracy in comparison to laboratory measurement [61].

S.M. Platt et al. investigated PM production in 2-stroke scooters. They focused on the primary and secondary organic aerosol formation (POA and SOA) and their potential health effects. SOA is being produced via atmospheric oxidation of precursor gases in the exhaust. According to their research conducted in 2014, oxidation of volatile organic compounds (VOCs) produces significant SOA with total OA 2.9 and 2.4 times higher than POA after ageing for idling and driving. Aged OA emissions are on average 53-771 times higher than laboratory studies on other vehicle types [14].

Also, a high amount of benzene, toluene and C2-C4 alkylated benzenes was observed in exhaust gas. Especially, the concentration levels of benzene in the raw exhaust were quite alarming (300,000$\mu g\, m^{-3}$ or 146 ppm), mostly observed during idling. Exposure of exhaust gas from the scooter vehicle during idling can be hence highly dangerous to health since benzene is considered carcinogenic. The reasons for such a high OA and aromatic emissions formation in 2-stroke scooters could be the addition of lubricant oils to the fuel, fresh fuel/air

mixture circulation in the chamber, frequent rich combustion and inefficient aftertreatment systems. The research showed that 2-stroke scooters are significant and, in some cities, the largest source of vehicular PM, toxic SOA and aromatic hydrocarbons. Implementing the restriction of 2-stroke scooters in some urban areas was suggested as a solution to this problem [14].

B. Giechaskiel et al. examined the uncertainties in emissions measurement of gaseous analysers and solid particle number (SPN) instruments for L-category vehicles. For their study from October 2019, they conducted several emissions measurements on a chosen moped while using both, sampling from the tailpipe and sampling from dilution tunnel. Gas analysers and SPN instruments with lower cut-off sizes of 4nm, 10 nm and 23 nm were used [62].

The main conclusion from the study was that dilution tunnel measurements with the open configuration, without any additional instruments sampling from the tailpipe, is more accurate for mopeds, especially for SPN measurements. It was also observed that the particles losses in the transfer tube from the vehicle to the dilution tunnel decreased the SPN by 30 %. Furthermore, exhaust flow was determined via three different methods: the difference between total and dilution air flow, the CO_2 tracer method and the carbon balance. The agreement of these methods was reasonable (with only 5 % uncertainty) [62]. It was also explained, that direct measurements of exhaust flow by flow meters are sensitive to the exhaust gas fluid conditions, such as flow rate, composition, temperature and pressure. In small one- or two-cylinder SI engines pulsating flows, especially during idling, are frequent. They can even cause reverse flow direction and for this reason, there are no exhaust flow meters for L-category vehicles and mostly indirect methods are used.

During their measurement, particle emissions below 23 nm were as high as those above 23 nm which is a current limit for passenger cars. Thus, lowering the size limit, standardized by the legislation, was suggested [62].

A.Konstses et al. conducted an experimental study of PM measurement on 30 Euro 1-4 L-category vehicles using a chassis dynamometer. The objective was to identify the most polluting sub-categories and to evaluate if Euro 5 will effectively control PM in this category. They found out that the vehicles with the highest particulate mass and particulate number above 23 nm are 2-stroke mopeds and diesel minicars. 4-stroke mopeds, motorcycles and quads emitted particulate mass emissions below the Euro 5 limit for passenger cars but they

reached SPN emissions up to 5 times higher than the Euro 6 (6×10^{11} km^{-1}). It was also observed that including SPN in the range of 10-23nm increases the emission levels up to 2.4 times compared to SPN of particles bigger than 23nm. Cold engine operation was told to be a major contributor to SPN emissions. The study suggested that L-category vehicles should be further monitored, and not only particulate mass limit but also the introduction of SPN limit should be required [63].

V. Císař performed experimental study regarding emissions measurement on Yawa 350 OHC Special as a part of his diploma thesis. He conducted 3 RDE routes which were then replicated in a laboratory on a chassis dynamometer. Euro 3 and WMTC cycle were also carried out to simulate driving conditions stated by the legislation. Gaseous emissions were then analysed by CVS, automobile PEMS and MiniPEMS, while the gas flow was measured by 2-inch EFM flowmeter. Additional RDE measure net was performed and emission concentrations during real driving operation of the vehicle were measured by MiniPEMS. It was observed that neither of the driving testing cycles carried out corresponds to the dynamic parameters of the real driving conditions of the vehicle. WMTC cycle turned out to be more dynamic than real driving conditions. During the flow measurement with the commercial flowmeter, pressure fluctuations in high amounts were present in the exhaust system which made it impossible to obtain correct data. It was explained that this problem occurs often when measuring exhaust gas flow of motorcycles with a small engine and small number of cylinders. It was suggested, that suitable technological solution such as prechamber or exhaust extension shall be found to eliminate this problem [64].

Conclusion of the theoretical part

In the theoretical part of the thesis, the principles of the combustion process of ICE, exhaust gas pollutants formation, legislation and emissions measurement were explained.

Most motorcycles use SI internal combustion engines and so they participate in air pollution in a similar way as four-wheel vehicles. The main harmful pollutants that are being formed in exhaust gas of ICE and that are regulated by the legislation are hydrocarbons (HC), oxides of nitrogen (NO_x) and oxides of carbon (CO, CO_2). There are also various pollutants that are not regulated such as particulate matter, greenhouse gases NO_2 and CH_4 and aldehydes. About formation of these unregulated pollutions, it is still not much known in the field of L-category vehicles.

Motorcycles fall in the vehicles of category L which can be further divided into 4 classes according to their maximal achievable speed and size. For each category, the emissions standards determine allowed emissions limit. Currently, newly produced motorcycles in Europe must satisfy Euro 5 requirements (see chapter 3.1).

To simulate driving conditions and measure exhaust gas pollutants formation in a laboratory environment, driving cycle WMTC is applied for motorcycles. There are several versions of the WMTC cycle according to the specific L-category class of the tested vehicle. The cycle is determined by the vehicle velocity profile and gear shifting points. The testing takes place on chassis dynamometer whose settings can be determined by performing coast-down test – a road test consisting of vehicle launch from a certain speed until it stops due to resistant forces. These forces are calculated and simulated by dynamometer settings.

Pollutants formation in exhaust gas can be measured simultaneously while the vehicle undergoes the driving cycle. The analysed exhaust gas sample can be either diluted or raw. For the diluted sample, special CVS for motorcycles should be used. When using standard CVS for passenger cars, it is problematic to measure the presence of pollutants that occur in the exhaust gas in small concentrations, because the sample is too much diluted. To solve this problem and to be able to detect also unregulated pollutants in small amounts, raw sampling can be used.

For this method of sampling, however, the gas flow must be measured simultaneously. This gas flow measurement proved to be very inaccurate when measuring directly by commercial flowmeters due to presence of pressure pulsations which can negatively influence the measured data. The presence of these pressure pulsations is quite common for vehicles with a small engine and a small number of cylinders and so usually indirect methods

are used. A static pitot tube is another way of exhaust flow measurement during raw sampling, but this methodology is still quite unexplored in the field of motorcycle exhaust gas flow measurement.

6 Experimental part

The goal of the experimental part of this thesis was to characterize the regulated and basic unregulated pollutants (including key properties of PM) from two in-use motorcycles. For this purpose, Yamaha XT 660R and Suzuki GSR 600 were chosen as the test vehicles. Method of raw exhaust sampling was selected for its advantage of detection of pollutants, present in the exhaust gas in small concentrations. Exhaust gas flow was measured by static pitot tube which is not a common method for flow measurement in the field of motorcycles testing. The goal was to obtain sustainable data for each motorcycle from the coast-down test, perform several testing driving cycles and to measure the formation of pollutants using convenient measuring analysers. The measured data were supposed to be evaluated and discussed. The measurement was to be validated by carbon balance and the effect of driving conditions on the pollutant's formation was to be discussed.

6.1 Methodology of the experiment

In the first part of the experiment, each motorcycle underwent coast-down testing conducted on a suitable test track. The coast-down data from both vehicles were obtained and evaluated in order to determine the road losses for dynamometer settings.

These settings were set on a chassis dynamometer Schenk 3604 located in the testing laboratory of Technical faculty of the Czech University of Life Sciences in Prague. Because the chassis dynamometer used for the experiment was primarily designed for automobiles, it was also necessary to compensate for the mass of a motorcycle. This was done by adding an extra torque to the dynamometer settings by electromotor connected to it. To sample exhaust gas, raw sampling method was used for gaseous pollutants measurement. Because of possible pressure fluctuations which could negatively influence the measurement of λ, a special tailpipe extension was designed and mounted onto each vehicle during the measurement.

Exhaust gas flow was measured simultaneously with the pollutants concentrations by a pitot tube located inside the tailpipe extension. Other ways of exhaust gas flow determination were used and will be described further.

For the simulation of real driving conditions, repeated in a laboratory environment, WMTC 3.2 driving cycle was used. To realize this cycle successfully, firstly gear shifting points thorough the cycle had to be calculated and both motorcycles had to be mounted on a chassis dynamometer separately.

Fuel BA 95 unleaded gasoline fuel with an octane number of 95, satisfying the standard CSN EN 228, was used for both motorcycles, which was suitable according to manufacturer requirements. The test driver followed the driving conditions of the WMTC cycle while the pollutants concentration, exhaust flow and other variables were measured simultaneously.

To characterize particulate emissions, total particle number and particle size distribution were measured after diluting part of exhaust gas sample with diluters.

The measured data were evaluated, and the results will be discussed in the last part of this thesis. The whole measurement was validated by carbon balance which will be also discussed further below.

A scheme of the performed experiment of emissions measurement with all measuring analysers can be seen in Figure 21.

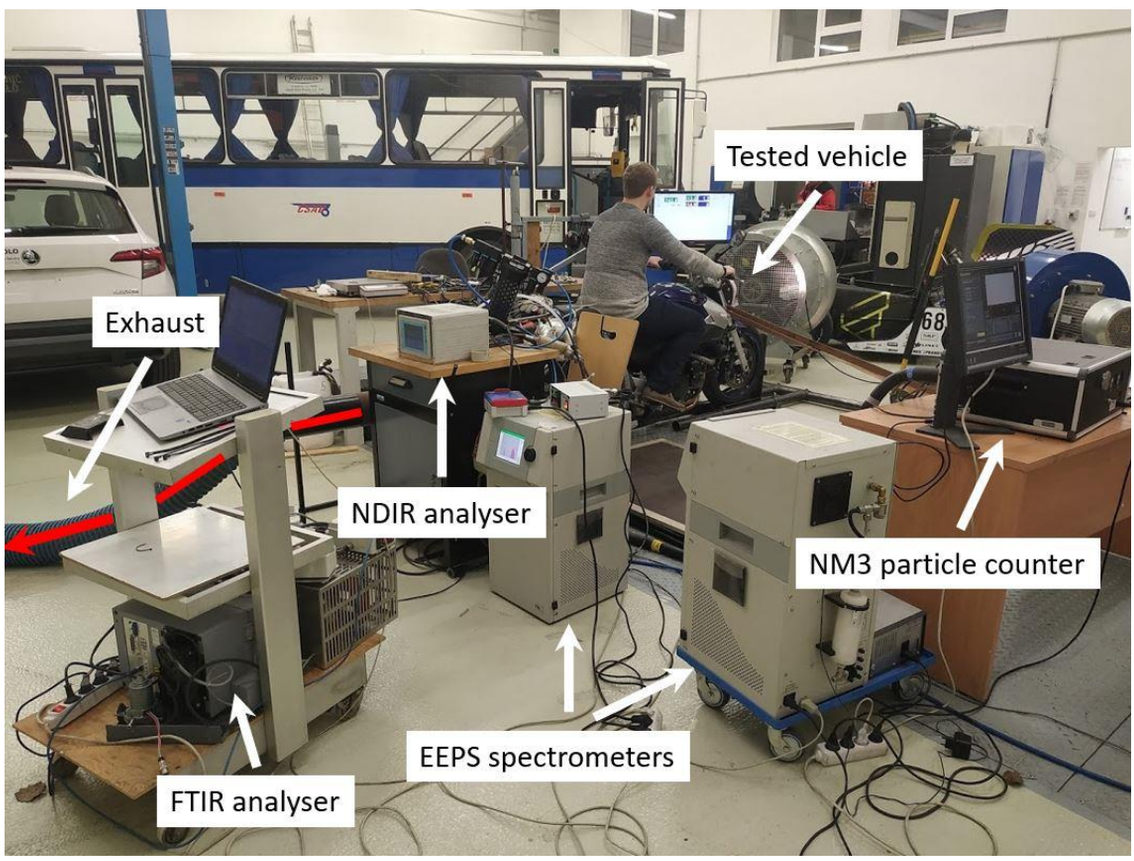

Figure 21 Scheme of the performed experiment of emissions measurement [author]

6.2 Tested vehicles

The measurement was conducted on two motorcycles, Yamaha XT 660R and Suzuki GSR 600. Yamaha XT 660R was chosen as a representative of motorcycles with one–cylinder engine while Suzuki GSR 600 contains 4 cylinders arranged in a line. Both of these vehicles were type approved to Euro 4 and equipped with a three-way catalyst. The main vehicle parameters of both motorcycles can be seen in Table 6.

Figure 22 Yamaha XT 660R [author]

Figure 23 Suzuki GSR 600 [author]

Table 6 Parameters of the tested vehicles [65] [66]

Parameter	Yamaha XT 660R	Suzuki GSR 600
Year of manufacture	2007	2008
Wet weight [kg]	181	183
Bore & Stroke [mm]	100 x 84	67 x 42.5
Number of cylinders	1	L4
Driven distance [km]	18 000	15 500
Maximal speed [km/h]	160	225
Fuel capacity [l]	15	16.5
Engine displacement [cm^3]	660	599
Max. power [kW]	35.3 (6000 rpm)	72 (12000 rpm)
Max. torque [Nm]	58.4 (5250rpm)	64.7 (9600 rpm)
Compression ratio	10:1	12.5:1
Type of cooling	Water	water

6.3 Measuring equipment

The scheme of the measurement on chassis dynamometer together with the measuring equipment can be seen in Figure 21. Throughout the whole experiment, the following measuring equipment was used.

- Chassis dynamometer Schenk 3604
- FTIR analyser Matrix MG-5
- NDIR Analyser VMK
- Particle spectrometer EEPS 3090
- NanoMet 3
- Digital scale Vibra AJ-6200 CE (max m = 6200g, accuracy 0.01g)
- Rotating disc diluter Testo MD19-3E
- A cascade of two ejector diluters Dekati DI-1000
- Static pitot tube
- Lambda probes (wide-band, one at each exhaust tailpipe)
- K-type thermocouples
- Coolers

During the testing cycles, several variables were being measured simultaneously. For each motorcycle, two lambda probes were used to determine the air/fuel ratio from each cylinder separately. Inside the tailpipe extension (see chapter 6.6) static-pitot tube was measuring the pressure difference by 3 pressure sensors. Next to pitot tube, K-type thermocouple was used to measure exhaust gas temperature. For the first motorcycle, the mass of fuel was measured simultaneously during the testing cycles by weighing. RPM of the vehicles was not measured directly but it was calculated from the pressure pulsations from pitot tube and from the intake manifold pressure.

6.4 Coast-down testing

The settings which simulate real road losses of each tested vehicle (such as aerodynamic drag, rolling resistance and grade resistance etc.) were determined from coast-down testing. The coast-down test consists of vehicle launch from a certain speed with the engine ungeared until the vehicle stops due to resistant forces (see chapter 5.2).

The measurement was conducted on a former military airport runway Pacov-Kamen. This location proved to be convenient for the coast-down testing thanks to a sufficient distance of two kilometres and good surface quality with only slight linear elevation. Only the west side of the runway was used for the measurement because it had a smaller elevation rate than the rest of the runway as it can be seen in Figure 24 (red curve). The testing was done in both directions to eliminate any influence of elevation and possible wind presence, and it was repeated 10 times for each motorcycle. During each test, instantaneous velocity in time was measured with GPS sensors with a frequency of 1Hz.

In order to satisfy the measurement conditions stated by the legislation (see chapter 5.2), it was necessary to compensate for the elevation which slightly exceeded allowed values in certain parts of the measurement. Because this cannot be simulated directly on the chassis dynamometer, values of acceleration from the measurement itself were slightly corrected to match the elevation change. Thanks to this correction and the fact that the measurement was done several times in both directions, the effect of this exceeded elevation was eliminated.

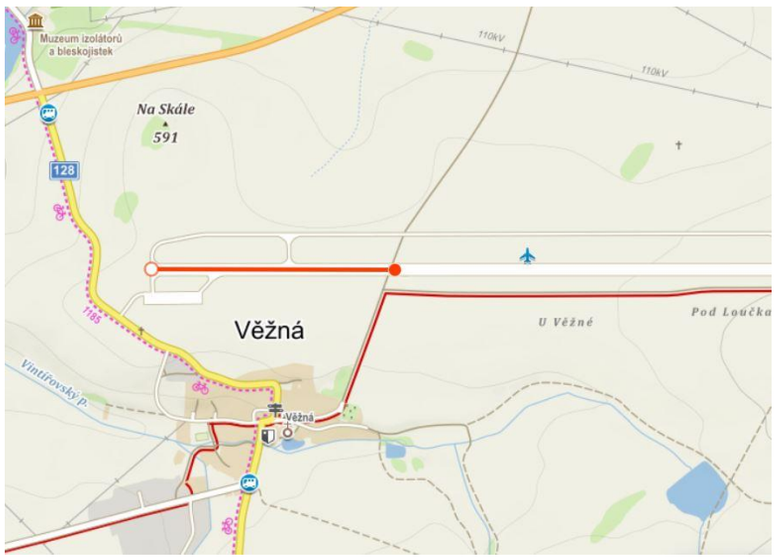

Figure 24 Location of coast-down testing [67]

6.4.1 Parameters of coast-down testing:

In order to satisfy required testing conditions, the following parameters were recorded:

- The temperature of ambient air: 7°C
- Interval of measured speeds for further evaluation: 100 – 0 km/h
- Ambient pressure: 98 kPa
- Total route distance: 2 km
- Driver weight: 75 kg
- Elevation: in total – 15 m (up to 1 % in some parts)
- Weight of a motorcycle with a driver before and after testing:
    - Yamaha XT 660 R – 256 kg
    - Suzuki GSR 600– 258 kg
- Wind speed: 2.22 m/s

Figure 25 Coast-down test [author]

Figure 26 Coast-down test [author]

6.4.2 Coast-down data evaluation and results

The measured data were evaluated in order to obtain corresponding coast-down curves for each motorcycle. These curves show a relation between velocity and acceleration and are plotted in Figure 27. Figure 28 shows road load forces as a function of velocity.

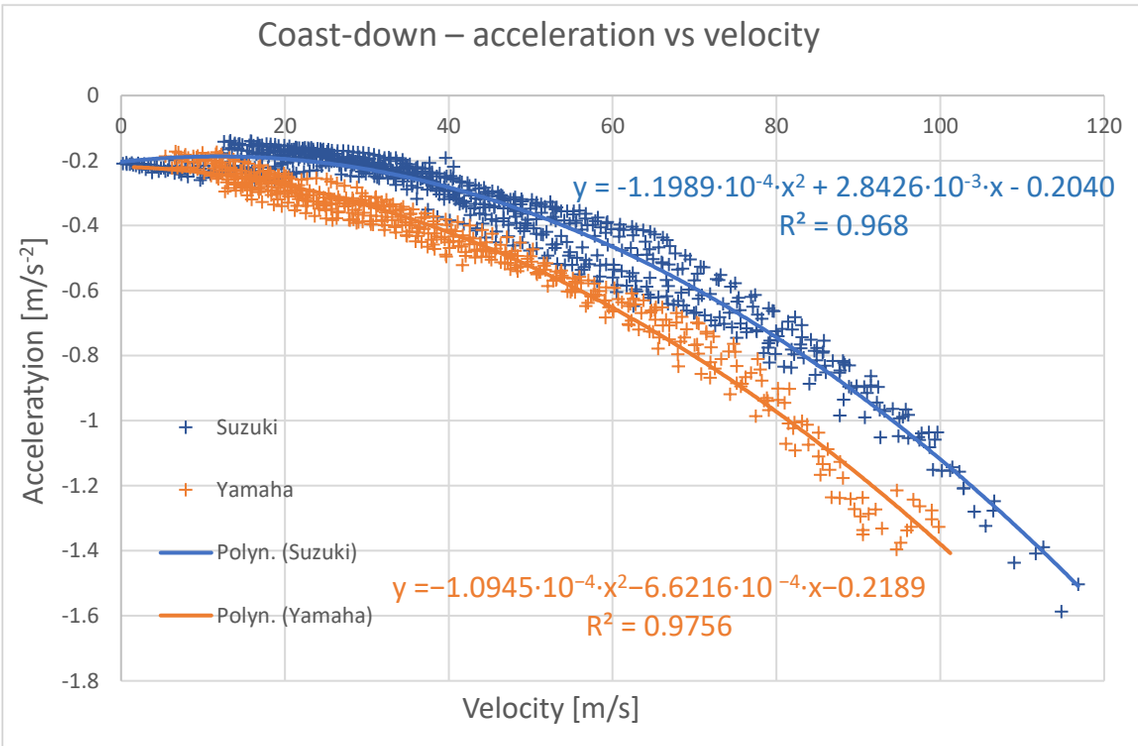

Figure 27 Coast-down test - acceleration as a function of velocity, R^2=coefficient of determination

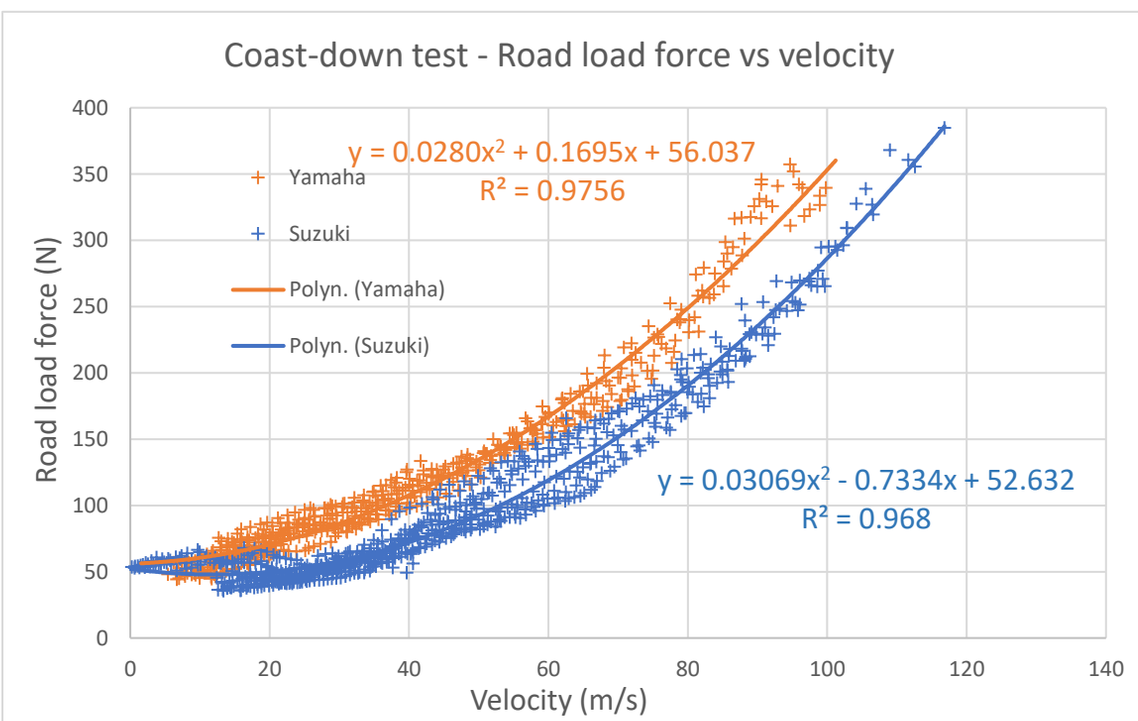

Figure 28 Coast-down test- road load force as a function of velocity, R^2=coefficient of determination

By using polynomial regression, the equations of these curves were calculated, and the following results were obtained:

Acceleration as a function of velocity for the first motorcycle (Yamaha XT 660R):

$$a_1(v) = -1.0945 \cdot 10^{-4} v^2 - 6.6216 \cdot 10^{-4} v - 0.2189$$

Acceleration as a function of velocity for the second motorcycle (Suzuki GSR 600):

$$a_2(v) = -1.1989 \cdot 10^{-4} v^2 + 2.8426 \cdot 10^{-3} v - 0.2040$$

The sum of road load forces *F(v)* can be described as a polynomial function of velocity, where *v* is instantaneous velocity and coefficients *a*, *b* and *c* determine the slope and shape of the curve. The general form of this equation is:

$$F(v) = av^2 + bv + c$$

From the evaluated data of acceleration and velocity and by application of Newton's second law, those coefficients were determined to be:

Table 7 Coefficients of the polynomial function of road load forces

	a	b	c
Yamaha XT 660R	0.02802	0.16951	56.0384
Suzuki GSR 600	0.03093	- 0.73339	52.632

These coefficients, which describe the sum of road load forces acting on the two vehicles in real conditions, were indirectly used for the settings of chassis dynamometer in a laboratory setup.

In Figure 29, a graph of velocity as a function of time is plotted. It is apparent, that there were higher load forces in the coast-down testing of Yamaha and hence the vehicle slowed down to a minimal speed faster.

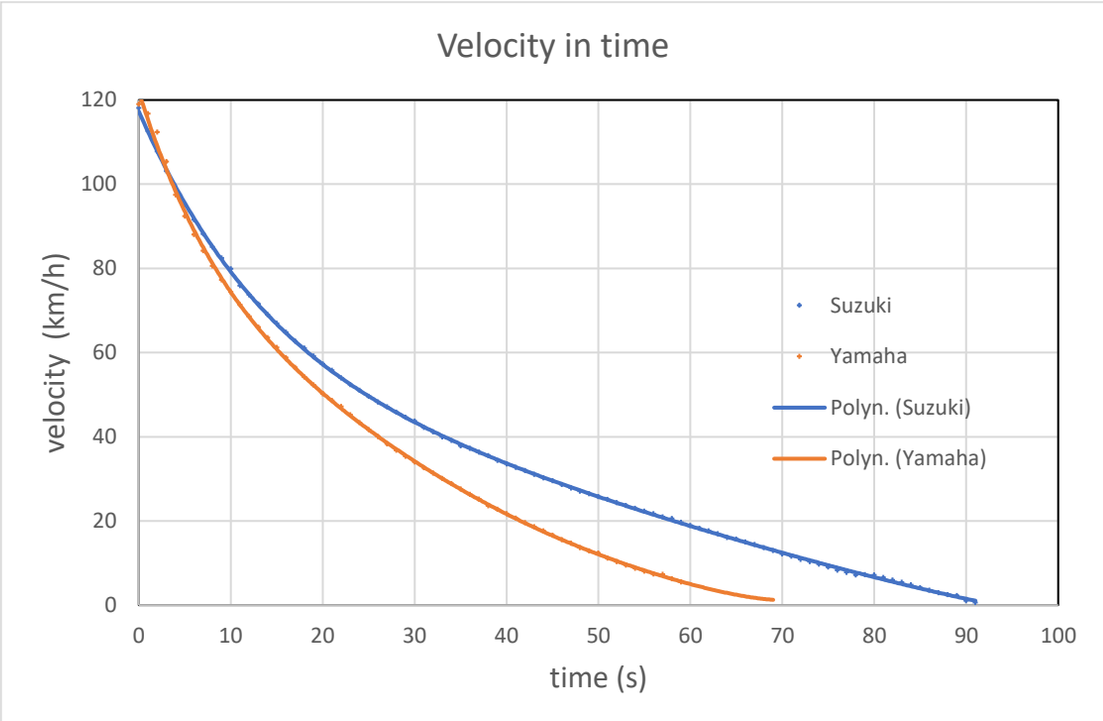

Figure 29 Velocity as a function of time

According to the type of chassis dynamometer used for the laboratory measurement, the road load characteristics were determined by the equation of dynamometer excited torque representing road load forces. The vehicle was being slowed down during the whole testing by this corresponding torque realized by the dynamometer.

It was also necessary to perform a coast-down test on a chassis dynamometer without any additional resistant forces. Then, the result coast-down curve was compared with the corresponding curve from the road coast-down measurement. Based on this comparison, the final dynamometer settings, which represent road load forces, were determined.

In Figure 30, an example of dynamometer final settings for Suzuki GSR 600 can be seen. The coast-down curves of the settings ("dyno 1 and 2") are compared with the target coast-down curve obtained from the road measurement. The green curve dyno 2 is the correct settings of the dynamometer but with cold tyres (hence slightly bigger resistances), while the blue curve is already the same settings with warmed tyres) As it can be seen the difference between the target curve and the two curves of dynamometer settings is very small and hence the settings of the dynamometer quite well represent real road load forces of the vehicle.

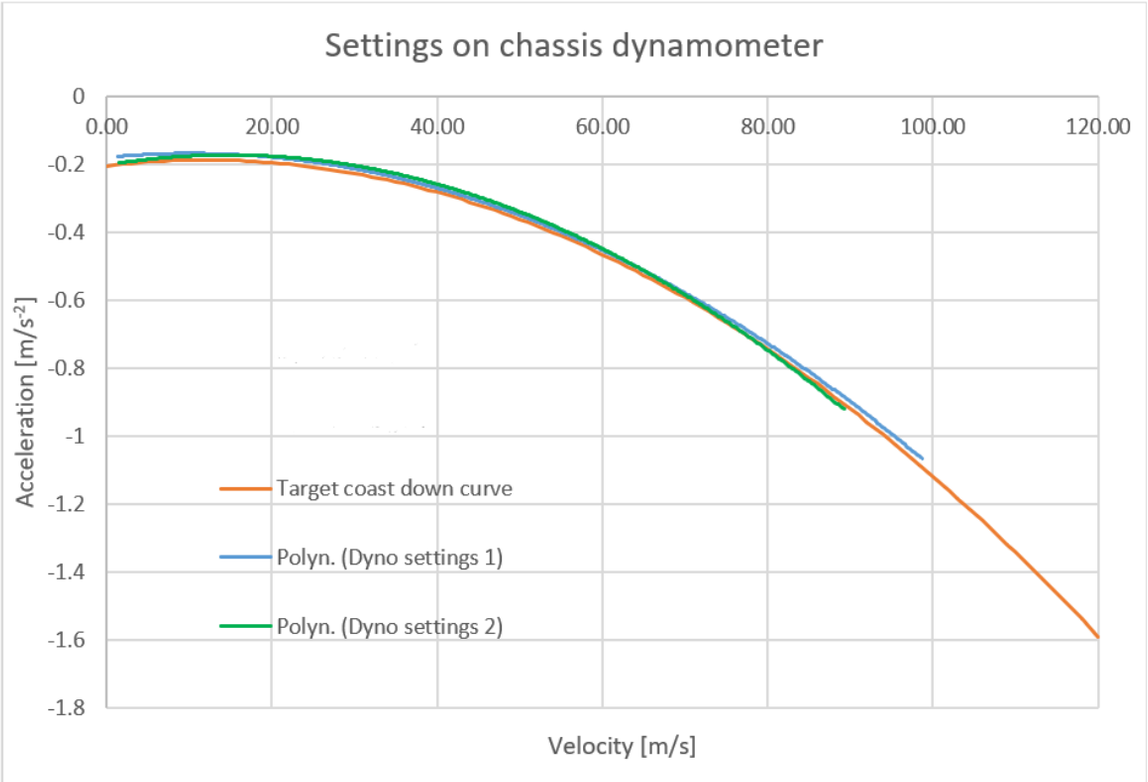

Figure 30 Final settings of the chassis dynamometer

6.5 Performing WMTC cycles on a chassis dynamometer

After evaluating the data from the coast-down testing, the vehicles were transported to a testing laboratory. Each motorcycle was separately mounted on the chassis dynamometer while sustaining direct contact of the back wheel with the dynamometer rollers. The vehicles had to be well secured in order to avoid sliding of the dynamometer during high speeds Cooling fans were placed in front of the tested vehicle to provide the flow of cooling air normally present during on-road operation.

The tailpipe extension was mounted on each vehicle and measuring instruments were all placed and set accordingly to measure desired variables. Before executing the WMTC cycles, steady-state operations were conducted to ensure the correct dynamometer settings and calibration of measuring instruments.

After all these preparations, the dynamometer settings obtained from the coast-down testing were set and the measurement during the simulation of the WMTC cycle could start.

Figure 31 Measurement on the chassis dynamometer [author]

The following measurements were performed:

Table 8 Performed emissions tests

Vehicle	Measurement	type of start	Gaseous emissions measurement	PM measurement
Yamaha XT 660R	1	cold	FTIR + NDIR raw	NM3 + EEPS
	2	warm	FTIR + NDIR raw	NM3 + EEPS
	3	warm	FTIR + NDIR raw	NM3 + EEPS
	4	warm	FTIR + NDIR raw	NM3 + EEPS
	5	warm	FTIR-diluted, NDIR raw	NM3 + EEPS
Suzuki GSR 600	6	cold	FTIR + NDIR raw	NM3 + EEPS
	7	warm	FTIR + NDIR raw	NM3 + EEPS
	8	warm	FTIR + NDIR raw	NM3 + EEPS
	9	warm	FTIR + NDIR raw	NM3 + EEPS
	10	warm	FTIR-diluted, NDIR raw	NM3 + EEPS

In all cases, the version of the applied driving cycle was WMTC 3.2, which corresponds to the current legislation and the class of both vehicles in the L-category. For the simulation of the testing cycle, according to the legislative requirements (see chapter 3.2.3), program ControlWeb was used. The testing driver was trying to replicate the required speed and gear selection shown on the screen in front of him. In the program, vehicles instantaneous velocity could be seen in comparison to the required velocity demanded by the legislation. The actual velocity had to be in the required interval of $\pm$ 3.2 $km.h^{-1}$ as it can bee seen in Figure 32.

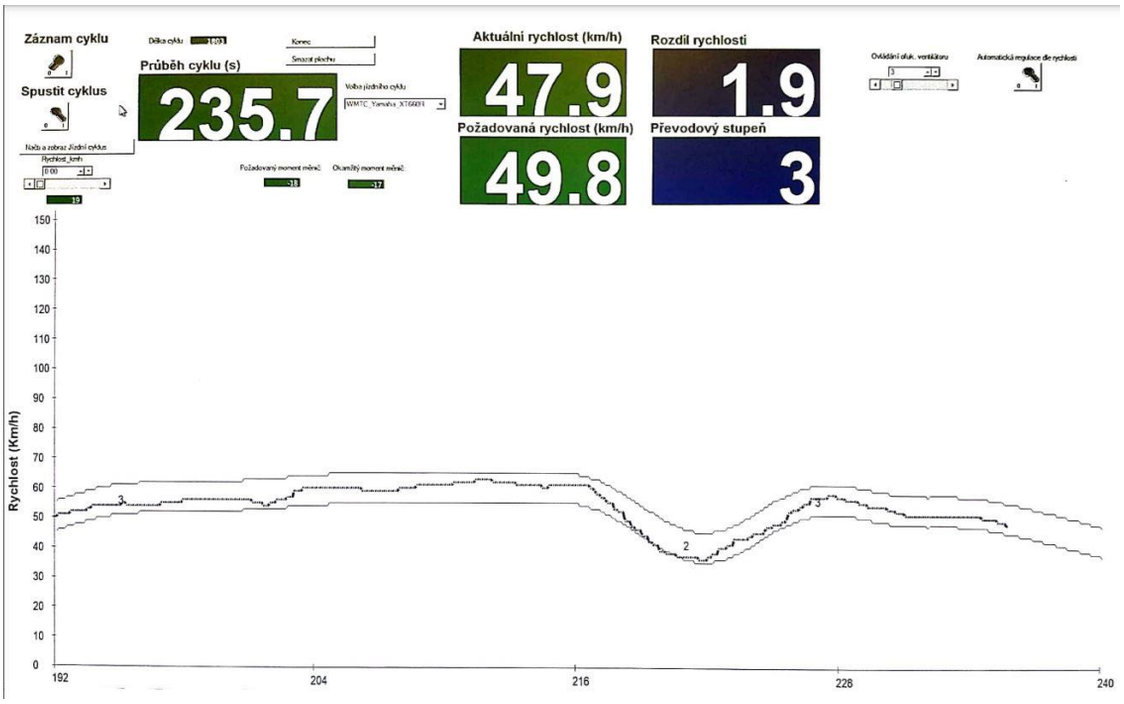

Figure 32 Actual speed in ControlWeb (y-axis = velocity [km/h], x-axis = time [s], [author]

The cycle itself proved to be difficult to reproduce especially during low rpm. Based on the calculated shifting points it was prescribed that the vehicle should work in second and third gear during very low speeds and rpm. The first part of the cycle had to be slightly adjusted in order to make it possible for both vehicles to replicate the speed profile.

In Figure 33 we can see the required speed profile of the WMTC cycle for the class 3.2 together with the corresponding gear selection. The green line shows the actual speed profile from the chassis dynamometer (measurement 8) and how well it replicated the required profile.

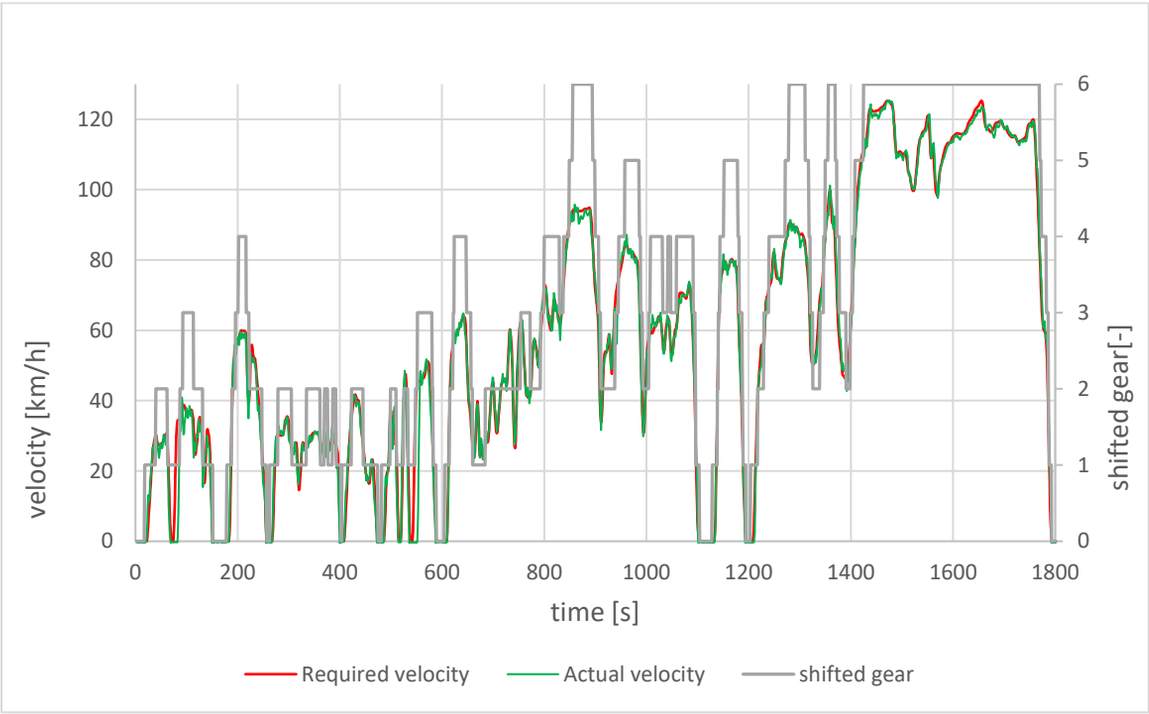

Figure 33 Speed profile of WMTC cycle

6.6 Exhaust gas sampling and flow measurement

To sample exhaust gas, the raw sampling method was used for gaseous pollutants measurement. This was done mainly to ensure possible detection of unregulated pollutants which often appear in exhaust gas only in small amounts. These small pollutants concentrations (in the order of a few dozens of ppm) would not be detectable by using a common method of diluting sampling with CVS system (see chapter 4.2.2). It is because the concentrations of desired compounds in such a diluted sample are too small to be detected by standard measuring instruments.

For evaluation of pollutants concentrations in a raw exhaust sampling method, it was necessary to measure instantaneous exhaust gas flow simultaneously. A static pitot tube was used for this direct flow measurement which turned out to be problematic. When a pitot tube was placed into a tailpipe directly, strong pressure fluctuations were present in the exhaust system which made the measurement of λ by the lambda probe distorted. These pressure fluctuations are quite common when measuring exhaust flow of raw gas of a single-cylinder engine (described in chapter 5.3). They are caused by strong pressure waves that travel to the tailpipe opening and are pushed back creating a vacuum inside the exhaust system. This leads to a suction of air inside the exhaust system which can cause reverse exhaust gas flow detected by the pitot tube as negative pressure difference.

To solve this problem, a special tailpipe extension was designed, manufactured, and mounted to the tailpipe before the measurement itself. (see Figure 34)

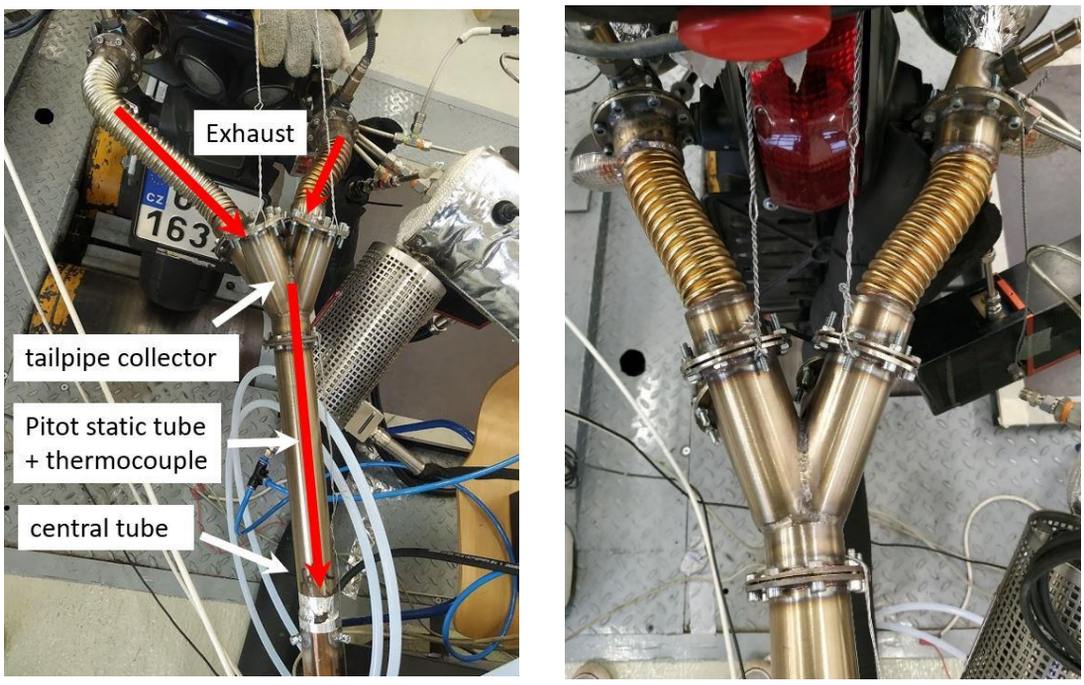

Figure 34 Tailpipe extension (mounted on Suzuki GSR 600 on the left and on Yamaha XT660 R on the right) [author]

This extension consists of sufficiently long central pipe equipped with a collector made from four openings. These openings were designed to fit onto the tailpipes of a motorcycle. Four openings were made in order to make this tool universal for all motorcycles with up to four tailpipes. Because the tested vehicles contained only 2 tailpipes, two of the openings of the collector had been temporarily closed and sufficiently isolated during the experiment. The length of the central pipe of the extension was made long enough to decrease the effect of pressure fluctuations on the measurement.

A small part of exhaust gas was collected from the tailpipe extension and sent directly to FTIR and NDIR analysers to measure gaseous emissions, while other part was sampled before the extension itself and sent to PM analysers.

The profile of exhaust gas temperature measured by the thermocouple plotted in the same graph together with the vehicle velocity can be seen in Figure 35. It is apparent that the exhaust temperature increases with velocity and it reaches maximal values of 340°C in the third sub-cycle (highway). The temperature had an effect on the formation of some pollutants as it will be described further.

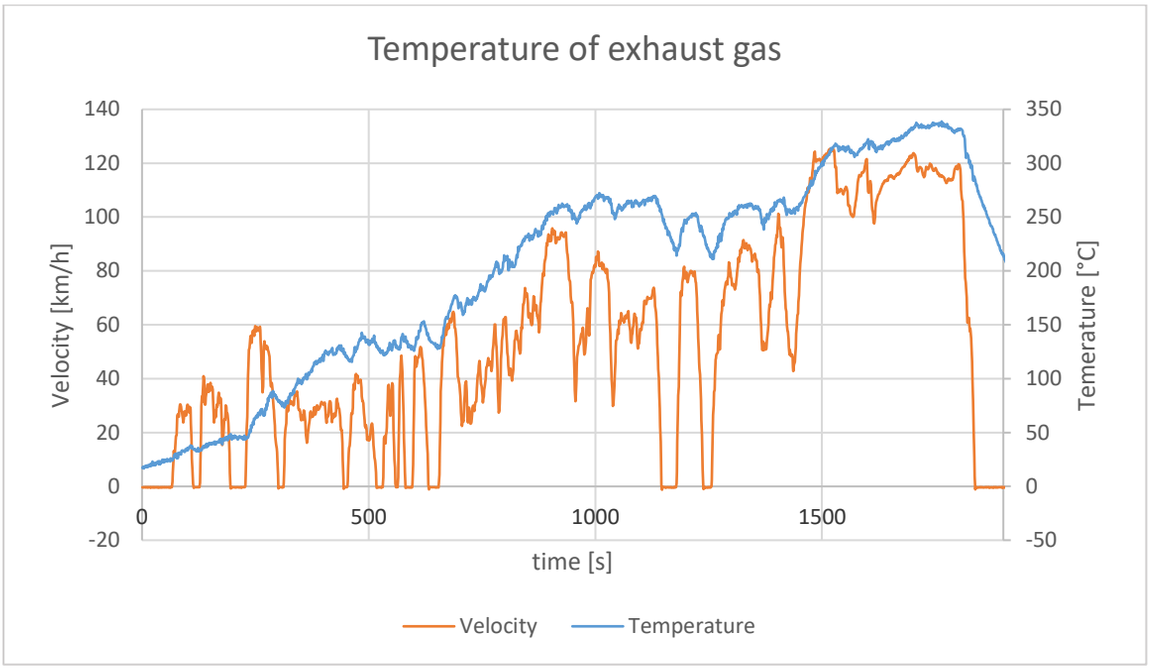

Figure 35 Temperature of exhaust gas

To obtain valid results from the exhaust flow measurement, the pitot tube had to be calibrated. The calibration itself was not part of this experimental work and so the procedure will be only described briefly.

Because there was no reference flow measurement, several methods of fuel consumption were compared between each other and the results were used to obtain pitot tube calibration coefficients. Before executing the testing cycles, additional steady-state operations were conducted while FTIR analyser was measuring the diluted sample from a full-flow dilution tunnel with a known constant flow and NDIR analyser raw sample. The same setup was done during one of the WMTC cycles for each motorcycle. The concentrations of exhaust gas components from both analysers were then multiplied by the respective exhaust flow (engine exhaust flow in the case of NDIR and total flow of diluted exhaust in the case of FTIR) and mass emissions flow rates (in g/s) were calculated. Total fuel consumption was then calculated from the cumulated mass emissions of carbon compounds from the exhaust (separately for FTIR and NDIR). The fuel consumption was also determined by weighing using gravimetry method and, in addition, by recording the volume of fuel poured inside the fuel tank. All results were then compared with the data obtained from the pitot tube and based on this comparison, calibration coefficients as a function of RPM were determined.

The pitot tube, used for this experiment, was measured with a frequency of 5kHz and had to be centred inside the pipe in order to measure the pressure difference correctly. For

the pressure difference, three pressure sensors with different frequencies and range were used, out of which only one was determined to be measuring reasonably and in a sufficient range (the design of the Pitot tube and the corresponding sensors was not part of this thesis).

From the pressure difference, instantaneous flow velocity $\boldsymbol{c_i}$ was calculated by using an equation (see chapter 4.4.1):

$$c_i = \sqrt{\frac{2 \cdot (p_t - p_s)}{\rho_i}} = \sqrt{\frac{2}{\rho_i}} \cdot \sqrt{\Delta p}$$

While $(p_t - p_s)$ was measured directly by the pitot tube, for the density ρ_i calculation we considered exhaust gas as an ideal gas and so ideal gas equation was used:

$$p \cdot V = n \cdot R \cdot T$$

By adjusting this equation, we could calculate instantaneous density ρ from the equation:

$$\rho_i = \frac{p_{bar}}{r \cdot T_i}$$

p_{bar} [kPa] = barometric pressure; p_{bar} = 101.325 kPa
r [J.kg.K^{-1}] = specific gaseous constant; r = 287.1 J.kg.K^{-1}
T_i [K] = instantaneous temperature

The assumption that exhaust gas is an ideal gas with the same parameters as air is a simplification which causes slightly inaccurate results, but the error is not bigger than a few tenths of percent. The instantaneous temperature T was measured by a thermocouple inserted inside the tailpipe extension.

In order to receive valid results, $\sqrt{\Delta p}$ had to be calculated for pressure data with a frequency of 5kHz and the results were then averaged to 500 Hz. The averaging had to be done after the calculation itself because of the nonlinearity of velocity caused by square root in the equation. Averaging the pressure values before this calculation would lead to incorrect results due to pressure fluctuations that were still present in the tailpipe system to some extent. From the calculated flow velocity, volumetric flow of exhaust gas $\dot{V}$ was be determined from the following equation:

$$\dot{V}_i = c_i \cdot S + \dot{V}_{i\_sampled}$$

$\dot{V}_i$ [$m^3.s^{-1}$] = instantaneous volumetric flow of exhaust gas
c_i [$m.s^{-1}$] = instantaneous velocity of exhaust gas
S [m^2] = surface area of the tailpipe extension main opening
$\dot{V}_{i\_sampled}$ [m^3s^{-1}] = volumetric flow sampled from the exhaust by analysers

From this, instantaneous mass flow of exhaust gas $\dot{m}$ was calculated as:

$$\dot{m}_i = \dot{V}_i \cdot \rho_{exhaust}$$

$\dot{m}_i$ [$kg.s^{-1}$] = instantaneous mass flow of exhaust gas
$\rho_{exhaust}$ [$kg.m^{-3}$] = exhaust gas density

For the further calculation of specific pollutant components, it is necessary to calculate also total molar flow of exhaust gas. This can be done by using the following equation:

$$\dot{n}_i = \frac{\dot{m}_i \cdot 1000}{M_{exhaust}}$$

$\dot{n}_i$ [$mol.s^{-1}$] = instantaneous molar flow of exhaust gas
$M_{exhaust}$ [$kg.mol^{-1}$]- molar mass of exhaust gas

To achieve accurate results, the molar mass of exhaust gas should be calculated by the sum of molar masses of all components of exhaust gas. A simplification was made when considering exhaust gas as an ideal gas with the same properties as air but the difference would be minimal.

An example from the instantaneous exhaust gas mass flow from the measurement of Yamaha XT 6060R with a warm start (measurement 3), calculated from the data of pressure difference from the pitot tube for Yamaha can be seen in Figure 36.

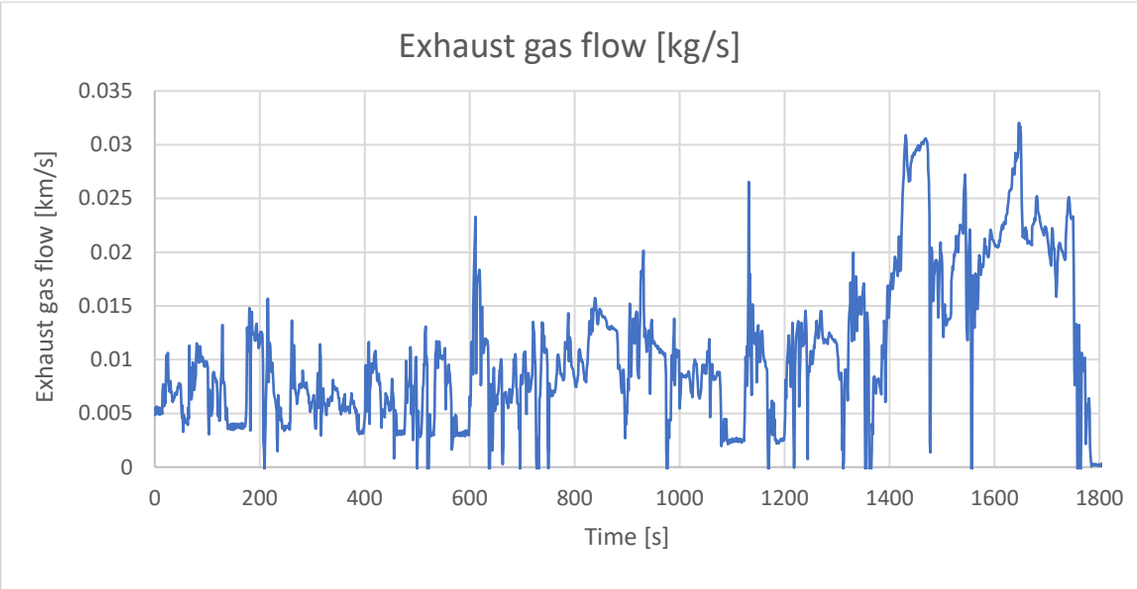

Figure 36 Exhaust gas flow from the pitot tube

It is apparent, that there were still some cases where the pressure fluctuations caused negative values of instantaneous mass flow, but the rate of these cases is very small, and it almost does not influence the final results. This shows that the pressure fluctuations can be resolved by using a pitot tube and a special tailpipe extension instead of commercial flowmeters. However, the sampling frequency must be sufficient (in this case 5kHz) and the square root from flow velocity calculation must be calculated for this frequency without averaging in order to obtain correct values. If smaller sampling frequency is used or averaging is done before the velocity calculation, the results are then strongly influenced by the pressure waves and often negative values of flow velocity are observed. Choosing the right sampling frequency and calibrating the pitot tube was however not part of the thesis work; these data were provided in and used in this work for further calculations.

6.7 Gaseous mass emissions measurement

Raw sample of exhaust gas from the tailpipe extension was collected and analysed by NDIR and FTIR analyser, both with a frequency of 1Hz. NDIR analyser was evaluating only concentrations of CO, CO2 and HC, while FTIR was examining concentrations of all regulated and unregulated gaseous pollutants detectable by this method. The output of both measuring analysers were concentrations of emissions components in the sample in units of ppm.

Comparison of CO and CO_2 concentrations from both analysers were used for their calibration. Concentrations of HC were only possible to detect by NDIR analyser. Mass flow of emissions components was calculated by equation:

$$\dot{m}_i^{(x)} = \frac{\dot{n}_{total} \cdot M^{(x)} \cdot C^{(x)} \cdot k}{10^6}$$

i [s] = time from the start of the testing cycle

x = specific emissions component

$\dot{m}_i^{(x)}$ *[g.s^{-1}] = mass flow of emissions component x*

$\dot{n}_{total}$ *[mol.s^{-1}] = total molar flow of exhaust gas*

$M^{(x)}$ *[kg.mol^{-1}] = molar mass of emissions component x*

$C^{(x)}$ *[ppm] = concentration of emissions component x (from FTIR)*

k = correction coefficient for pitot tube

The total mass of produced emissions component during a testing cycle was calculated from:

$$\sum_{i=1}^{n} \dot{m}_i^{(x)}$$

n [s] = duration of testing cycle (1800s for WMTC cycle)

It was successfully managed to measure concentrations of basic regulated pollutants: CO_2, CO, HC and NO. With the application of the method of FTIR spectroscopy, it was not possible to evaluate NO_2 concentrations due to the indistinctive absorbing spectrum. However, the formation of NO_2 in the case of SI engines is negligible as it was explained in chapter 2.1.1 and so it was considered NO_x concentrations same as NO concentration.

In Table 9 mass emissions of regulated pollutants and CO_2 from all performed measurements from FTIR analyser are displayed. The data of hot start measurement represent the average of the four hot start cycles performed. with hot start were averaged accordingly.

Table 9 Mass emissions of regulated gaseous pollutants from FTIR analyser

Vehicle	Type of start	CO_2 [g/km]	CO [g/km]	NOx [g/km]	HC [g/km]
Yamaha XT 660R	Hot	128	6.26	0.288	0.348
	Cold	129	7.18	0.289	0.331
Suzuki GSR 600	Hot	111	5.29	0.114	0.357
	Cold	118	2.56	0.117	0.355
Euro 4 limit	-	-	1.14	0.090	0.17
Euro 5 limit	-	-	1.00	0.060	0.100

Concentrations of several unregulated pollutants were also detected by FTIR analyser and their mass emissions were calculated. From these pollutants, the following were observed in nonnegligible amounts: Ammonia (NH_3), methane (CH_4), formaldehyde (HCHO) and Nitrous oxide (N_2O). The mass emissions of these components can be seen in Table 10.

Table 10 Mass emissions of unregulated gaseous pollutants

Vehicle	Type of start	NH_3 [mg/km]	CH_4 [mg/km]	HCHO [mg/km]	N_2O [mg/km]
Yamaha XT 660R	hot	275	58.4	5.6	9.7
	cold	266	61.3	5.8	10.5
Suzuki GSR 600	hot	91	53.3	6.9	7.1
	cold	33	46.1	8.2	4.6

Mass emissions of regulated pollutants CO, NO_x and HC, calculated for both tested vehicles, are graphically illustrated in Figures 37-39. HC emissions of both vehicles were very similar but due to only NDIR analyser performing this measurement and no reference measurement, those results are not validated. Other results were mostly different for each vehicle as expected. In most cases, Yamaha XT 660R produced higher values of mass emissions of both regulated and unregulated gaseous pollutants. The only exception was formaldehyde and NO_2 emissions for cold start. A big effect on this had a different richness of the mixture of each motorcycle during the combustion process. Another reason could be a different technological solution of TWC present in both vehicles and regulation of air/fuel ratio.

As there were 4 measurements with a warm start for each vehicle, the values of mass emissions were averaged, and standard deviations were calculated. These deviations are listed in Table 11 and they are also plotted graphically in Figures 37-39 (vertical line in the top of the columns). These standard deviations show good repeatability of the measurement as separate WMTC cycles and gaseous analysis brought similar results.

Table 11 Standard deviations of gaseous mass emissions

	CO_2 [g/km]	CO [g/km]	NO [g/km]	HC [g/km]	NH_3 [mg/km]	CH_4 [mg/km]	HCHO [mg/km]	N_2O [mg/km]
Yamaha XT 660R	4.26	1.12	0.019	0.084	14	2.6	1.7	0.9
Suzuki GSR 600	2.68	0.77	0.007	0.061	19	3.1	1	0.6

The relative standard deviations (the ratio of a standard deviation to the corresponding mean value, expressed in percent) are plotted in Table 12.

Table 12 Relative standard deviations of gaseous mass emissions in percent

	CO_2 [%]	CO [%]	NO [%]	HC [%]	NH_3 [%]	CH_4 [%]	HCHO [%]	N_2O [%]
Yamaha XT 660R	3.33	17.89	6.60	24.14	5.09	4.45	30.36	9.28
Suzuki GSR 600	2.41	14.56	6.14	17.09	20.88	5.82	14.49	8.45

(When comparing the mass emissions for CO, NO_x and HC stated by Euro 4 limit, according to which they were homologated, it was observed, that none of the vehicles exhibited emissions lower than the limit. The same applies to current Euro 5 limits. Yamaha XT 660R exceeded Euro 5 limits for CO emissions by 591 %, NO_x emissions by 395% and HC emissions by 249 %. Mass emissions from Suzuki GSR 600 were a bit lower but still, they exceeded the limits for CO by 306 %, for NO_x by 100 % and for HC by 268 %.

The reason for this can be the fact, that both motorcycles were probably type-approved using a different cycle than WMTC which was not so dynamic and hence the mass emissions obtained from this cycle were lower. Another effect could have been wear and ageing of the engine and aftertreatment system.

When comparing mass emissions from the cold and hot start, it was observed that there was not such a big difference. In most cases, the results were similar for both types of start. An exception can be seen in the mass emissions of CO, which reached higher values for cold start. This was unexpected as there is often more CO formed when the TWC is not yet warmed up. The reason for this was a richer mixture present during the cold start, which decreased the efficiency of TWC. The temperature of the catalyst not to be such an important factor as the mixture was mostly rich during higher loads and hence TWC could not work efficiently.

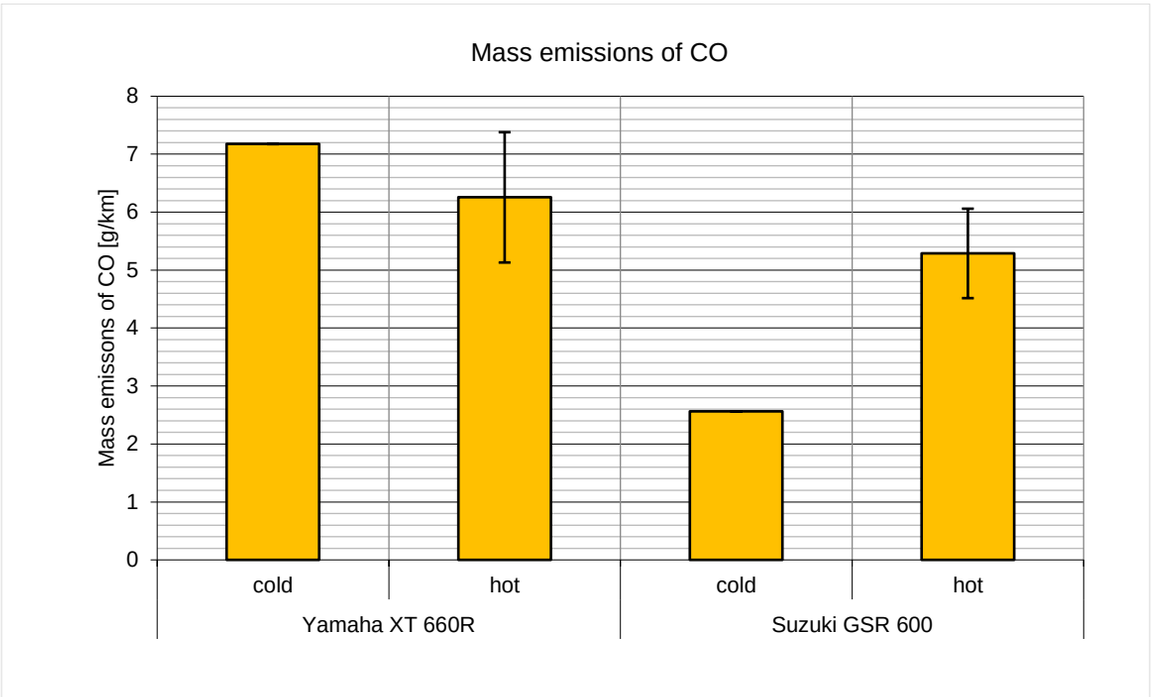

Figure 37 Mass emissions of CO

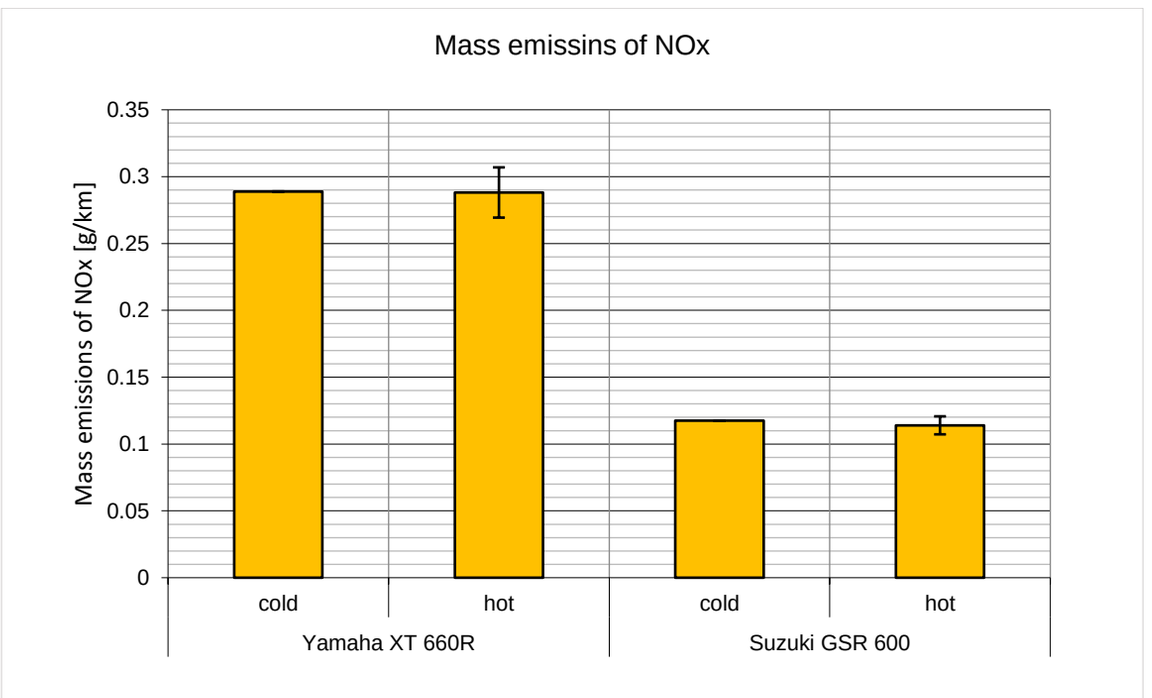

Figure 38 Mass emissions of NO_x

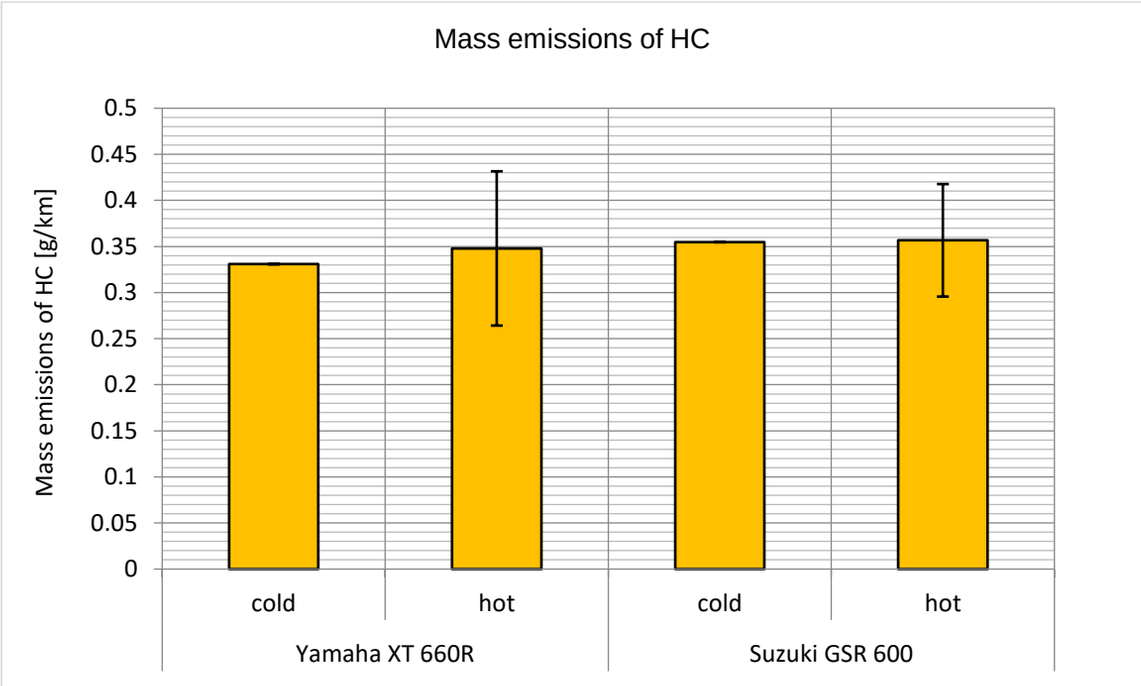

Figure 39 Mass emissions of HC

As it was explained in chapter 2.1.2, CO emissions depend strongly on the air/fuel ratio λ. This dependence can be seen in Figure 40 which show CO formations in time together with actual λ measured by the lambda probe during Measurement 3. It is apparent, that the most of CO is emitted when the engine works in rich conditions and also during higher speeds where these rich conditions are frequently present. A similar effect was observed for production of HC and for unregulated pollutants NH_3, N_2O and slightly for CH_4 (see Figures 41 and 42) However, for these unregulated pollutants, there are other factors that influence their formation.

What is alarming is the amount mass emissions of Ammonia, especially those emitted from Yamaha XT 660R, as they reached values of 275 mg/km for a hot-start and 266 mg/km for a cold start. As it was mentioned in chapter 2.3, Ammonia is known to be a toxic gas that contributes to secondary PM formation and so high concentrations in the environment are undesirable.

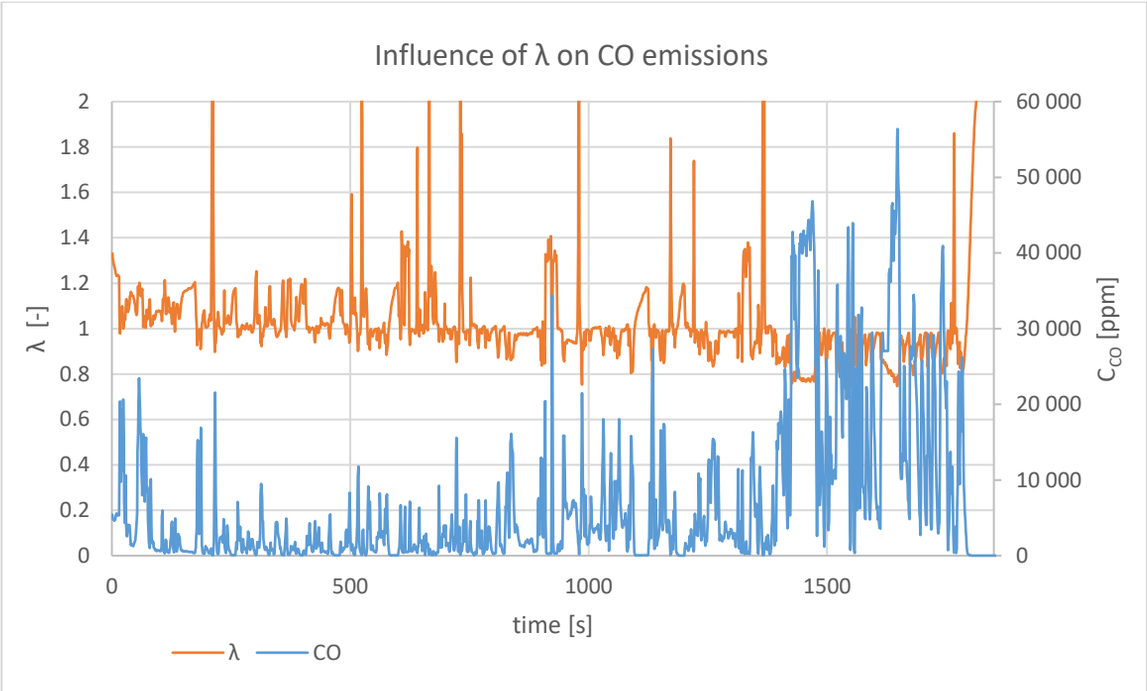

Figure 40 Influence of λ on CO emissions

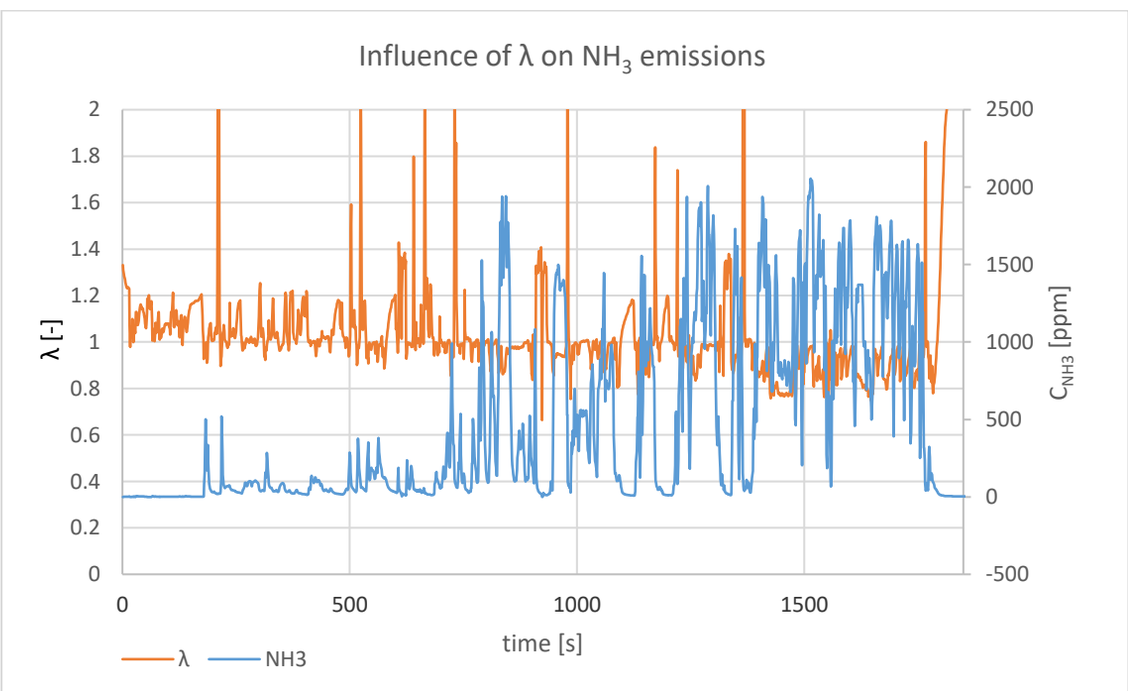

Figure 41 Influence of λ on NH_3 emissions

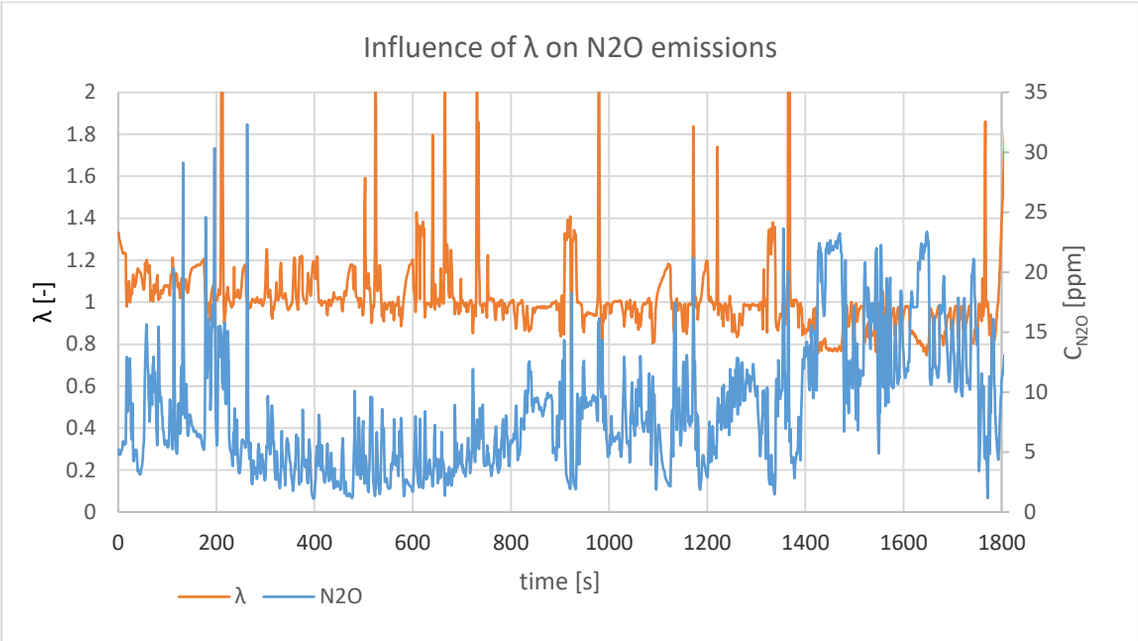

Figure 42 Influence of λ on N_2O emissions

Other unregulated emissions did not occur in such high amounts but still, their concentrations were not found negligible. It was also observed that concentrations of formaldehyde were much higher during the first part of the cycle with a cold start, which was caused by cold TWC which has not yet attained its operating temperature. This phenomenon can be seen in Figure 43 (Measurement 1).

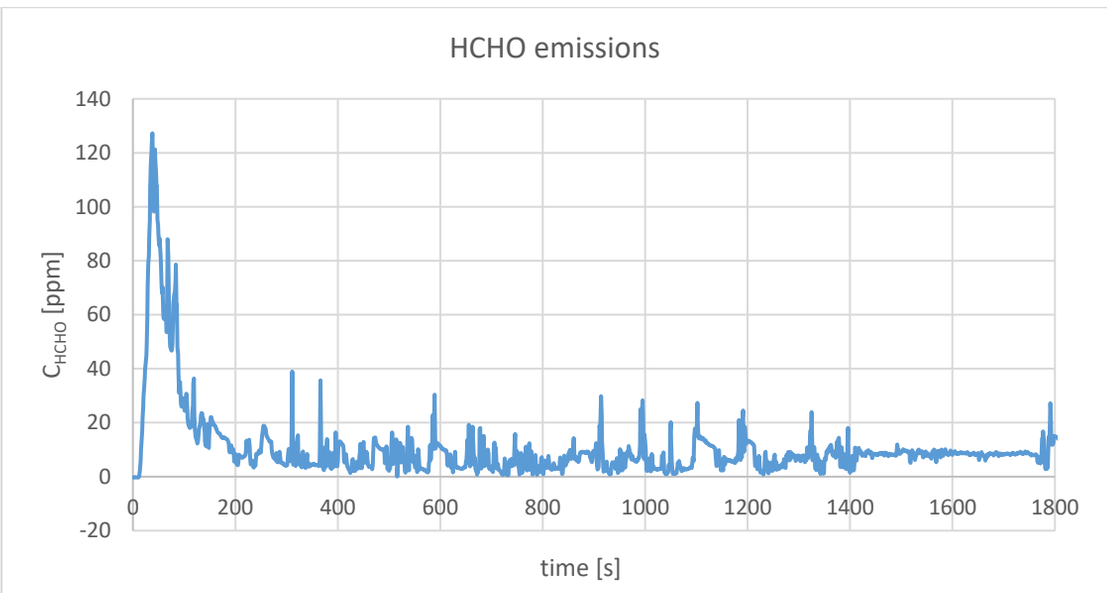

Figure 43 HCHO emissions

6.8 Particulate emissions measurement

Part of exhaust gas was collected from the tailpipe (before the extension) and it was analysed by NanoMet3 (NM3), another part was diluted with air by diluters and then analysed by two Engine

Exhaust Particle Sizers (EEPS). NM3 and both EEPS analysers were used for evaluating Particle number (PN) of particles bigger than 23nm, while particle mass (PM) was measured only by NM3. NM3 analyser was measuring only non-volatile particles, EEPS both volatile and non-volatile particles. The two EEPS were also able to measure the size distribution of particles present in the sample. While NM3 has its own sample dilution and conditioning system, the EEPS analysers can work only with a diluted sample and so two diluters were used for this purpose, rotating disc diluter for one EEPS and a cascade of ejector diluters for the other EEPS.

The comparison of the two diluters and of EEPS with NM3 was a part of a separate study aimed at the characterization of particles from SI engines and is not reported on in detail in this thesis. The values of PN from both EEPS were averaged. The results of PN from EEPS were compared between each other and together with results of PM they are plotted in Table 13. All results were also compared by the current Euro 6 limit for SI passenger cars.

Table 13 The results of PN and PM of particles bigger than 23nm

Vehicle	Type of start	PN from NM3 [-/km]	PN from EEPS [-/km]	PM from NM3 [mg/km]
Yamaha XT 660R	hot	$2.80 \cdot 10^{12}$	$1.26 \cdot 10^{12}$	0.930
	cold	$2.85 \cdot 10^{12}$	$2.05 \cdot 10^{12}$	0.839
Suzuki GSR 600	hot	$7.55 \cdot 10^{11}$	$3.65 \cdot 10^{11}$	0.077
	cold	$1.38 \cdot 10^{12}$	$7.40 \cdot 10^{11}$	0.250
Euro 6 limit for passenger cars		$6 \cdot 10^{11}$		4.5

It is apparent, that the PN results varied between both types of analysers. It was expected that NM3 analyser would give lower PN values for particles bigger than 23nm because it counts only solid particles, however, the opposite was observed as can be seen in Figure 45.

This could be possibly caused because of a slower decrease in particles concentration signal for NM3. When the concentration of particles rapidly decreased, EEPS reacted much faster. NM3 recorded this change much later and so more particles, than those present, were added to PN. This can be seen in Figure 44 where, as an example, instantaneous

concentrations of particles from both, EEPS and NM3 from the beginning of the measurement 10 are plotted.

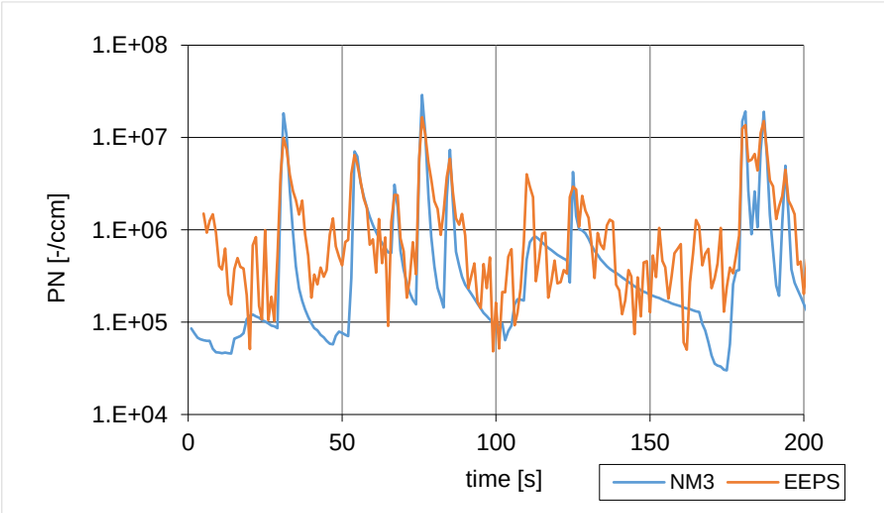

Figure 44 Concentrations of particles from EEPS and NM3

Another reason for lower PN values obtained from EEPS analysers could be the fact, that even though NM3 is supposed to measure only particles bigger than 23nm, it detects also smaller particles with smaller efficiency (for particles of size 10nm this efficiency is around 10 %). When there is a high amount of particles smaller than 23nm in the sample, even with this small efficiency of detection, it can strongly influence the final results. In Figure 46, where the size distribution of particles is shown, it can be seen, that most of the particles were indeed smaller than 23nm.

Yamaha XT 660R proved to be much worse particulate emitter concerning both PN and PM. As there is currently no limit of particulate emissions for L-category vehicles, the data were compared with the current Euro 6 limit for passenger cars. From this comparison, we can see that PN limits were exceeded (except for the hot start of Suzuki GSR 600), while PM values remained below the Euro 6 limits. This shows that most of these particles were smaller and lighter as is also confirmed from size distribution measurement from EEPS, described below.

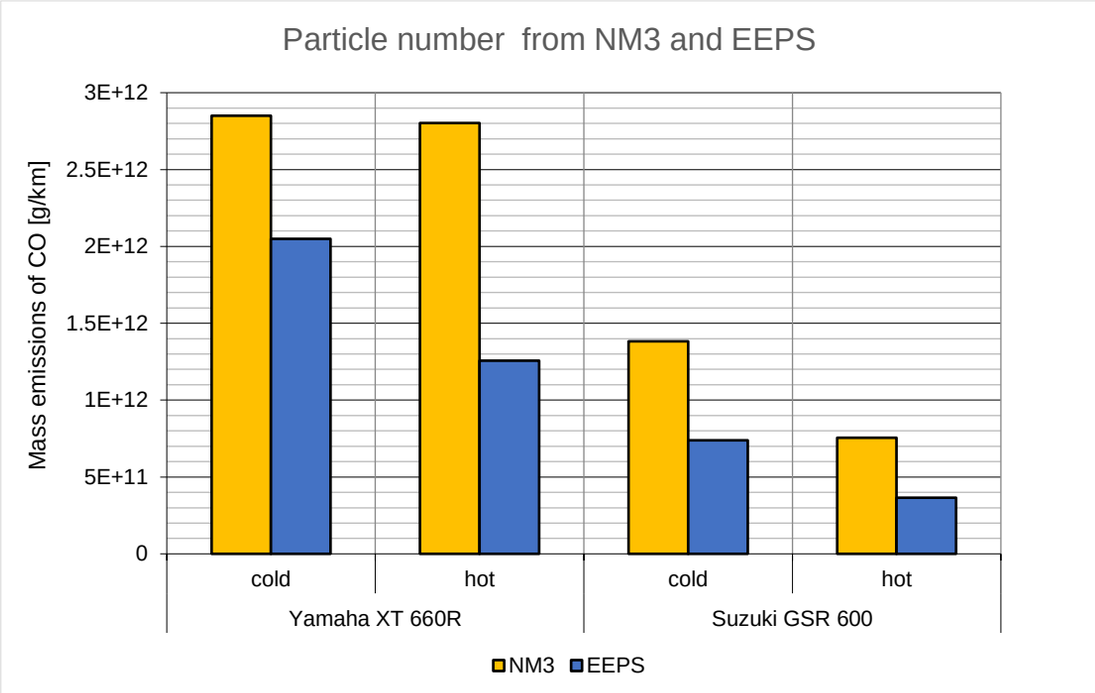

Figure 45 Results of PN from NM3 and EEPS analysers

Because the measured values of PN and PM are not negligible, it shows that particulate emissions from motorcycles is a relevant topic which should be further examined and discussed.

EEPS were also collecting data of size distribution of particles. From these data, an example of the size distribution of particles from Measurement 8 (Suzuki GSR 600, hot start) is shown in Figure 46.

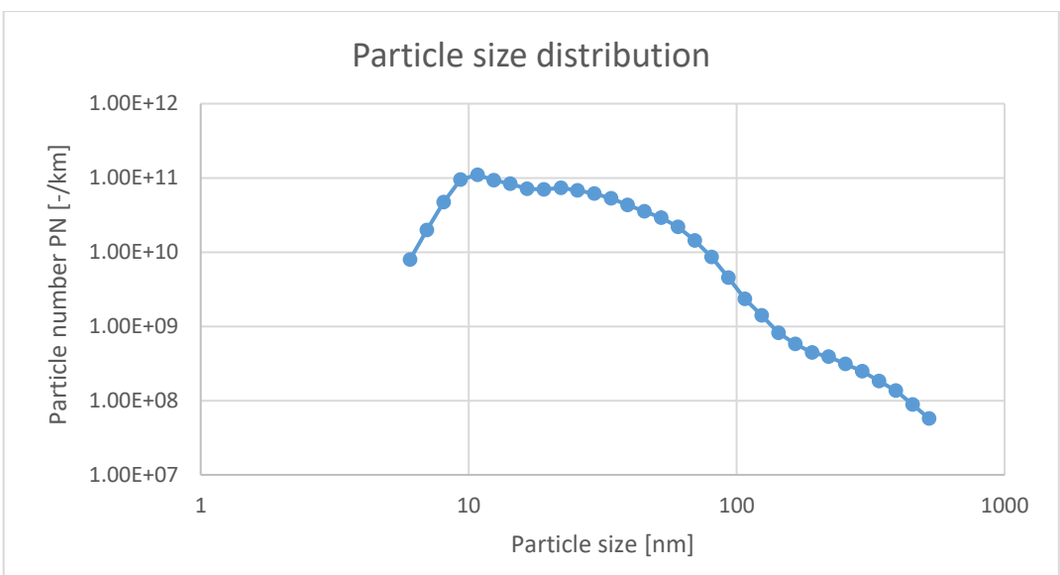

Figure 46 Particle size distribution

It can be observed that there is a significant number of particles smaller than 23nm, specifically, most of the particles produced in this measurement were those with a diameter around 10nm. This shows that counting only particles bigger than 23nm is not sufficient as it is known that smaller particles are even more harmful as it was explained in chapter 2.1.4. Similar was observed for all measurement performed.

PN number of all particles detected by EEPS, including those of size between 5 and 23nm was also evaluated additionally to see how strongly this would affect the PN results. In Table 14, PN of both, particles bigger than 23nm (PN23) and particles bigger than 5nm (PN5) from all measurements can be seen.

Table 14 PN5 and PN23 results

Vehicle	Type of start	PN23	PN5	(PN23/PN5)
Yamaha XT 660R	hot	1.26E+12	1.62E+12	77
	cold	2.05E+12	2.66E+12	77
Suzuki GSR 600	hot	3.65E+11	1.12E+12	33
	cold	7.40E+11	1.72E+12	43

It is apparent, that considering also particles smaller than 23nm increases the total PN significantly. The difference between PN5 and PN23 was bigger for Suzuki GSR 600, in the case of hot start, PN23 represented only 33% of total PN including particles smaller than 23nm (PN5). Further data evaluation and calculations would be needed to examine this aspect deeper.

6.9 Validation of mass emissions measurement

To validate the measurement of mass emissions, the law of conservation of mass was applied. Fuel consumption was calculated from emissions measured by both FTIR and NDIR analysers and compared with reference measurement of the fuel consumption. The effects of oil absorption and a fraction of unburned fuel were considered negligible as they would not influence the results significantly.

Instantaneous mass of fuel was calculated by the following equations, the first one is valid for FTIR analyser and the second one for NDIR.

$$\dot{m}_i^{(fuel)} = \frac{\frac{M_C}{M_{CO2}}\dot{m}_i^{(CO2)} \cdot \frac{M_C}{M_{CO}}\dot{m}_i^{(CO)} + \frac{M_C}{M_{CH4}}\dot{m}_i^{(CH4)} + \frac{M_C}{M_{CH2O}}\dot{m}_i^{(CH2O)}}{0.866}$$

$$\dot{m}_i^{(fuel)} = \frac{\frac{M_C}{M_{CO2}}\dot{m}_i^{(CO2)} \cdot \frac{M_C}{M_{CO}}\dot{m}_i^{(CO)} + \frac{6M_C}{M_{C6H14}}\dot{m}_i^{(C6H14)}}{0.866}$$

$\dot{m}_i^{(fuel)}$ *[kg.s^{-1}] = instantaneous mass flow of fuel*

$\dot{m}_i^{(x)}$ *[kg.s^{-1}] = instantaneous mass flow of specific component x*

M_x *[kg.mol^{-1}] = molar mass of specific component x*

0.866 = proportion of carbon in a gasoline fuel

C_6H_{14} *= hexane, equivalent of HC*

The total mass of consumed fuel calculated from the concentrations from both analysers was calculated by:

$$\sum_{i=1}^{n} \dot{m}_i^{(fuel)}$$

A fuel tank of the first motorcycle (Yamaha XT 660R) was unmounted from the vehicle and inserted onto a digital scale, where fuel consumption was measured (simultaneously with gaseous emissions analysis) by a gravimetry method. It was not possible to unmount fuel tank from the second motorcycle (Suzuki GSR 600) and so a different technique of fuel consumption estimation was used. Before the start of a testing cycle, the value of fuel surface height inside the fuel tank was marked and after the end of the cycle, a specific amount of fuel was poured inside the tank until it reached the same height. The mass of poured fuel was then evaluated from weighing a canister containing the fuel.

The amount of consumed fuel for each cycle obtained from these two methods was set as a reference and it was compared with the data obtained gaseous analysis and pitot tube.

There were no significant differences between the results from the pitot tube and the reference. The deviation between the results and the reference was in all cases smaller than 5 percent. This validates both the flow measurement with a pitot tube and the determination of mass emissions.

Also, as a result of this comparison for Yamaha XT 660R, where continuous weighing of the fuel was possible, calibration coefficients as a function of RPM were also determined.

In Table 15 the results of this validation are presented. In all cases, the amount of consumed fuel measured by reference methods was higher than the value calculated from the analysers. FTIR/NDIR deviation are the differences between total fuel consumption measured over the test as determined from FTIR/NDIR measurement and fuel consumption obtained from a reference measurement.

Table 15 Comparison of fuel consumption from gaseous analysis and the reference measurement

Vehicle	Type of start	Reference [g]	FTIR [g]	NDIR [g]	FTIR deviation [%]	NDIR deviation [%]
Yamaha XT 660R	cold	1267	1251	1247	-1.2	-1.6
	warm	1272	1274	1272	-2.7	-2.9
Suzuki GSR 600	cold	1132	1092	1110	-4.3	-1.9
	warm	1142	1116	1121	-2.3	-1.9

In Figure 47, we can see the mass of consumed fuel, calculated from both: mass flow (from pitot tube), and continuous weighing of the fuel tank from measurement 2 (Yamaha XT 660 R), chosen as an illustrating example (from measurement 3). We can also observe that in faster sub-cycles, fuel consumption increases which corresponds to the real driving conditions.

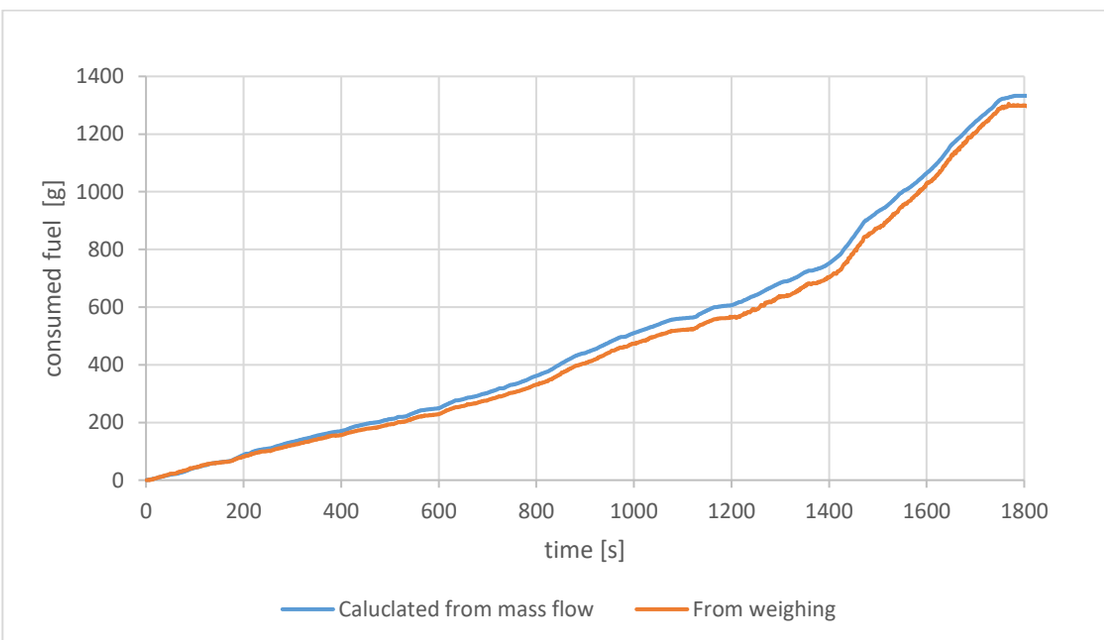

Figure 47 Comparison of fuel consumption calculated from the mass flow and obtained from weighing

6.10 Summary of the results

In Table 16, the results of mass emissions of all regulated and some unregulated gaseous pollutants are presented. CO_2, CO and HC were analysed by NDIR analysis, while the rest of the pollutants except HC were analysed by FTIR spectroscopy. WMTC 3.2 was used for all measurements as a testing cycle according to the class of tested vehicles. Measurement with a hot start was repeated four times for each motorcycle, including one additional testing with FTIR analysing a diluted sample. Good repeatability of gaseous analysis for a hot start was observed.

Table 16 Results of mass emissions of gaseous pollutants

Vehicle	Yamaha XT 660R		Suzuki GSR 600	
Type of start	Hot (N=4)	Cold	Hot (N=4)	cold
CO_2 [g/km]	128 ± 5	129	111 ± 3	118
CO [g/km]	6.26 ± 1.12	7.18	5.29 ± 0.77	2.56
NO [g/km]	0.288 ± 0.019	0.289	0.114 ± 0.007	0.117
HC [g/km]	0.348 ± 0.084	0.331	0.357 ± 0.061	0.355
NH_3 [mg/km]	275 ± 14	266	91 ± 19	33
CH_4 [mg/km]	58.4 ± 2.6	61.3	53.3 ± 3.1	46.1
HCHO [mg/km]	5.6 ± 1.7	5.8	6.9 ± 1	8.2
N_2O [mg/km]	9.7 ± 0.9	10.5	7.1 ± 0.6	4.6

Mass emissions from regulated pollutants CO, NO_x and HC were compared with a Euro 4 limit used for homologation of the tested motorcycles and current Euro 5 limit for L-category vehicles and in all cases, both limits were exceeded several times. Extremely high mass emissions of Ammonia were observed for both vehicles but especially for Yamaha XT 660 R. which emitted on average 0.27 g/km.

Measurement of particulate emissions was also conducted. A diluted sample was analysed by particle counter NanoMet3 (NM3) to measure PM and two Engine Exhaust Particle Sizers (EEPS) were used to evaluate particle size distributions and total particle number concentrations. The results of PM and PN measurement are summarized in Table 17. The results showed, that PN values would exceed the current limit Euro 6 for passenger cars with SI. PM values remained under the current limit which shows that most of the particles present in the exhaust were small and light which was also confirmed by size distribution data.

PN of particles bigger than 5nm was also measured and it is apparent that smaller particles influence total PN significantly and neglecting them leads to distorted results.

Table 17 Results of particulate emissions measurement

Vehicle	Yamaha XT 660R		Suzuki GSR 600	
Type of start	hot	Cold	hot	Cold
PM from NM3 [mg/km]	0.930	0.839	0.077	0.251
PN23 from NM3 [-/km]	$2.80 \cdot 10^{12}$	$2.85 \cdot 10^{12}$	$7.55 \cdot 10^{11}$	$1.38 \cdot 10^{12}$
PN23 from EEPS [-/km]	$1.26 \cdot 10^{12}$	$2.05 \cdot 10^{12}$	$3.65 \cdot 10^{11}$	$7.40 \cdot 10^{11}$
PN5 from EEPS [-/km]	$1.62 \cdot 10^{12}$	$2.66 \cdot 10^{12}$	$1.12 \cdot 10^{12}$	$1.72E \cdot 10^{12}$

It shall also be mentioned that the emissions tend to be higher during real-driving conditions thanks to various factors (such as maximal speed, gear-shift strategy, driver's behaviour, ambient conditions, ageing of aftertreatment system etc). In order to get more representative results than those from the laboratory measurement, RDE testing could be also conducted, but it would be complicated due to space demands of the analysers.

The mass emissions measurement was validated by a carbon balance, where the fuel consumption was recorded during the measurement by a reference method. By comparing total fuel consumption from this reference method with fuel consumption calculated by a carbon balance, similar results were obtained and the deviation between these two approaches was in all cases smaller than 5 percent.

CONCLUSION

The goal of this thesis was to characterize the emissions of regulated and basic unregulated pollutants from two in-use motorcycles.

In the first part of this thesis, general principles of the combustion process, emissions formation, aftertreatment technologies, legislative requirements and emissions measuring methods were described in order to build sufficient theoretical basis for the experiment of pollutants measurement.

In the second part, the experiment was conducted, and its methodology was explained. Two vehicles, Yamaha XT 660 R and Suzuki GSR 600, were tested, obtained data have been evaluated, and the results were discussed and compared with emissions limits Euro 4 and Euro 5 stated by the legislation in Europe.

Coast-down testing was conducted, and the evaluated results used for the optimal settings of chassis dynamometer to mimic the road losses. Exhaust sampling system and a tailpipe extension were installed and exhaust gas flow, concentrations of gaseous pollutants and key properties of PM were measured. Problematics of flow measurement of small engines was discussed, and the correct approach was explained and conducted. It was successfully managed to obtain exhaust flow velocity when using static pitot tube, inserted in a tailpipe extension and evaluating the data with a frequency of 5kHz. Such an approach of gas flow measurement is something unique in case of L-vehicles applications and it expands current general knowledge in this area. Both vehicles underwent WMTC 3.2 testing cycle with both cold and hot start. The type of start turned out not to be such an important factor. WMTC was shown to be problematic to replicate accurately, especially due to the inconvenient gear change strategy for low RPM.

Mass emissions of regulated gaseous pollutants of hydrocarbons (HC), carbon monoxide (CO) and nitrogen oxides (NO_x) and also unregulated emissions of ammonia (NH_3), methane (CH_4), formaldehyde (HCHO) and nitrous oxide (N_2O) were examined. Both vehicles exceeded Euro 4 and the current Euro 5 limit of regulated pollutants several times. Mentioned non-regulated pollutants were observed in non-negligible amounts and principles of their formation were also discussed. Extremely high mass emissions of Ammonia were observed for both vehicles but especially for Yamaha XT 660R. which emitted on average 0.28 g/km. Examining unregulated gaseous emissions of L-category vehicles is something that is still not much known about and so the results are beneficial as an introduction to this field.

Measurement of particulate emissions was also conducted. A diluted sample was analysed by particle counter NanoMet3 and two Engine Exhaust Particle Sizers to evaluate particulate matter characteristics. The results showed that PN values exceeded the current Euro 6 limit for passenger cars. PM values remained under the limit which shows that most of the particles present in the exhaust were small and light which was also confirmed by size distribution data. Most of the particles were those of size around 10nm. When comparing PN of particles bigger than 23nm and PN of all particles detectable (>5nm), a significant difference was observed. This suggests that also those particles smaller than 23nm should be regulated in the future for all vehicles, as they are proved to be even more harmful than the bigger ones. Yamaha XT 660R proved to be worse particulate emitter as values of both PM and PN were several times higher than those from Suzuki GSR 600.

The whole experiment was validated by carbon balance. The fuel consumption calculated from data from FTIR and NDIR analysers brought similar results as a reference measurement, with the difference being only in the range from 1.2 to 4.2 %.

The experiment showed that the formation of both regulated and unregulated gaseous pollutants from L-category vehicles is a relevant problem which shall be further examined. Also, particulate emissions, which are currently not even regulated by legislation, were observed to be extremely high, even higher than current limits for passenger cars in terms of PN. The currently applied regulations do not cover all harmful substances that are created during the combustion of these vehicles. Also, RDE testing for L-category vehicles is a relevant topic as laboratory testing cannot reproduce the real driving conditions precisely, and the real emissions could be even higher for the two tested vehicles. This work brought a contribution to the topic of emissions measurement of L-category vehicles and the results suggest that further research in this field is definitely needed.

List of References

[1] Worldwide emissions standards- passenger cars and light duty vehicles. *Delphi technologies* [online]. [cit. 2020-10-08]. Available at: https://www.delphi.com/sites/default/files/2019-05/2019-2020%20passenger%20car%20&%20light-duty%20vehicles.pdf

[2] Heywood, John B. *Internal combustion engine fundamentals*. Second edition. New York: Mcgraw-Hill Education, 2018. ISBN 978-126-0116-106.

[3] Bayless, David. Combustion. In: *Ohio University Web* [online]. Ohio, USA, 2010 [cit. 2020-10-08]. Available at: https://www.ohio.edu/mechanical/thermo/applied/chapt.7_11/chapter11.html

[4] *Air-fuel ratio, lambda and engine performance* [online]. [cit. 2020-10-07]. Available at: https://x-engineer.org/automotive-engineering/internal-combustion-engines/performance/air-fuel-ratio-lambda-engine-performance/

[5] Suarez-Bertoa, Ricardo. *On-road emissions of passenger cars beyond the boundary conditions of the real-driving emissions test* [online]. 2009 [cit. 2020-09-22]. ISBN 0013-9351. Available at: https://www.sciencedirect.com/science/article/pii/s001393511930369x?via%3dihub

[6] Emissões E. Sistemas de tratamento de gases de escape. *Le Auto Leiridiesel Group* [online]. [cit. 2020-12-08]. Available at: https://ldauto.net/emissoes-e-sistemas-de-tratamento-de-gases-de-escape

[7] Kohler, Eduard a Rudolf Flierl. *Verbrennungsmotoren: motormechanik,berechnung und auslegung des hukolbenmotors*. 4.auflage. Germany: vieweg, 2006. ISBN 10 3-528-43108-3.

[8] Hromádko, Jan. *Ekologické aspekty provozu spalovacích motorů* [online]. In: . [cit. 2020-10-08]. Available at: https://oppa-smad.tf.czu.cz/?q=system/files/10.pr_.ppt

[9] Oxid uhelnatý. *Integrovaný registr znečišťování* [online]. [cit. 2020-10-07]. Available at: https://irz.cz/repository/latky/oxid_uhelnaty.pdf

[10] Takáts, Michal. *Měření emisí spalovacích motorů*. CTU:Prague, 1997. ISBN 80-01-01632-3.

[11] *Integrated science assessment (ISA) for oxides of nitrogen – health criteria (final report, January 2016)* [online]. U.S. Enviromental Protection Agency, Washington DC [cit. 2020-10-07]. Available at: https://cfpub.epa.gov/ncea/isa/recordisplay.cfm?deid=310879

[12] Oxidy dusíku (NOx/NO2). *Integrovaný registr znečišťování* [online]. [cit. 2020-10-07]. Available at: https://irz.cz/repository/latky/oxidy_dusiku.pdf

[13] Diesel exhaust particle size. *Dieselnet* [online]. [cit. 2020-12-08]. Available at: http://courses.washington.edu/cive494/dieselparticlesize.pdf

[14] Platt, S. and I. Pieber. Two-stroke scooters are a dominant source of air pollution in many cities. *Nature Communications* [online]. [cit. 2020-12-08]. Available at: https://doi.org/10.1038/ncomms4749

[15] Overview of greenhouse gases. *United states environmental protection agency search* [online]. [cit. 2020-12-08]. Available at: https://www.epa.gov/ghgemissions/overview-greenhouse-gases

[16] Rodríguez, Felipe and Jan Dornoff. Beyond NOx: emissions of unregulated pollutants from a modern gasoline car. *The International Coucil on Clean Transportation* [online]. [cit. 2020-10-08]. Available at: https://theicct.org/publications/beyond-nox-emissions-unregulated-pollutants

[17] Formaldehyde and cancer risk. *National Cancer Institute* [online]. [cit. 2020-10-09]. Available at: https://www.cancer.gov/about-cancer/causes-prevention/risk/substances/formaldehyde/formaldehyde-fact-sheet

[18] Von Rueden, Stefanie. *Exhaust and emission aftertreatment systems explained: aftertreatment systems affect vehicle efficiency and performance.* [online]. [cit. 2020-10-08]. Available at: https://www.vehicleservicepros.com/vehicles/powertrain/emissions-fuel-efficiency/article/20982808/exhaust-and-emission-aftertreatment-systems-explained

[19] Pereda-Ayo, Beñat and Juan González-Velasco. *NOx storage and reduction for diesel engine exhaust aftertreatment* [online]. [cit. 2020-12-08]. Available at: https://www.intechopen.com/books/diesel-engine-combustion-emissions-and-condition-monitoring/nox-storage-and-reduction-for-diesel-engine-exhaust-aftertreatment

[20] The three-way catalytic converter. *The open university* [online]. [cit. 2020-10-08]. Available at: https://www.open.edu/openlearn/ocw/mod/oucontent/view.php?printable=1&id=2492

[21] Voncken, jJack. Recovery of Ce and La from spent automotive catalytic converters. *Critical and rare earth elements* [online]. [cit. 2020-10-08]. Available at: https://www.researchgate.net/publication/337203725_recovery_of_ce_and_la_from_spent_automotive_catalytic_converters

[22] Leroy, t. A j. Chauvin. Air path estimation for a turbocharged SI engine with variable valve timing. *American Control Conference* [online]. [cit. 2020-10-08]. Available at: https://www.researchgate.net/publication/224718205_air_path_estimation_for_a_turbocharged_si_engine_with_variable_valve_timing

[23] Geivanidis, Savas. *Study on possible new measures concerning motorcycle emissions final report* [online]. [cit. 2020-10-26]. Available at: https://ec.europa.eu/docsroom/documents/1840/attachments/1/translations/en/renditions/native

[24] Bielaczyc, Piotr and Joseph Woodburn. *Trends in automotive emission legislation: impact on LD engine development, fuels, lubricants and test methods: a global view, with a focus on WLTP and RDE regulations* [online]. [cit. 2020-10-08]. Available at: https://doi.org/10.1007/s40825-019-0112-3

[25] He, Hui and Lingzhi Jin. A historical review of the U.S. vehicle emission compliance program and emission recall cases. *The International Council on Clean Transportation* [online]. [cit. 2020-10-08]. Available at: https://theicct.org/sites/default/files/publications/epa-compliance-and-recall_icct_white-paper_12042017_vf.pdf

[26] Euro standards. *ACEA* [online]. [cit. 2020-10-08]. Available at: https://www.acea.be/industry-topics/tag/category/euro-standards

[27] Document 02014r0134-20180320. *Commission delegated regulation EU* [online]. [cit. 2020-10-08]. Available at: http://data.europa.eu/eli/reg_del/2014/134/2018-03-20

[28] Chung, Dennis. *What you need to know about euro 5 emission standards for motorcycles* [online]. [cit. 2020-10-09]. Available at: https://www.motorcycle.com/features/what-you-need-to-know-about-euro-5-emission-standards-for-motorcycles.html

[29] Eu: cars and light trucks. *Dieselnet* [online]. [cit. 2020-10-08]. Available at: https://dieselnet.com/standards/eu/ld.php

[30] Pavlovic, j., B. Ciuffo, G. Fontaras, V. Valverde and A. Marrota. How much difference in type-approval CO2 emissions from passenger cars in Europe can be expected from changing to the new test procedure (NEDC vs. WLTP)?. *Science direct* [online]. [cit. 2020-10-08]. Available at: https://doi.org/10.1016/j.tra.2018.02.002

[31] Fontaras, Georgios. The difference between reported and real-world CO2 emissions: how much improvement can be expected by WLTP introduction?. *Research gate* [online]. [cit. 2020-10-08]. Available at: https://www.researchgate.net/publication/317420498_the_difference_between_reported_and_real-world_co_2_emissions_how_much_improvement_can_be_expected_by_wltp_introduction

[32] Peter, Mock. The WLTP: how a new test procedure for cars will affect fuel consumption values in the EU. *The international council on clean transportation* [online]. [cit. 2020-10-08]. Available at: https://theicct.org/sites/default/files/publications/icct_wltp_effecteu_20141029.pdf

[33] Plotkin, Stephen E. Examining fuel economy and carbon standards for light vehicles. *Joint transport research centre* [online]. [cit. 2020-10-08]. Available at: http://www.internationaltransportforum.org/jtrc/discussionpapers/discussionpaper1.pdf

[34] ECE 15 + EUDC / NEDC. *Dieselnet* [online]. [cit. 2020-12-08]. Available at: https://dieselnet.com/standards/cycles/ece_eudc.php

[35] Worldwide harmonized light vehicles test cycle (WLTC). *Dieselnet* [online]. [cit. 2020-12-08]. Available at: https://dieselnet.com/standards/cycles/wltp.php

[36] Steven, Heinz. Worldwide harmonised motorcycle emissions certification procedure: draft technical report. *Rwtüv fahrzeug GMBH institute for vehicle technology* [online]. [cit. 2020-12-08]. Available at: https://www.unece.org/fileadmin/dam/trans/doc/2003/wp29grpe/trans-wp29-grpe-45-inf09e.pdf

[37] Worldwide harmonized motorcycle emissions certification/test procedure (WMTC) informal group. *UNECE* [online]. [cit. 2020-12-08]. Available at: https://unece.org/worldwide-harmonized-motorcycle-emissions-certificationtest-procedure-wmtc-informal-group

[38] Bischoff, Gregor. *PEMS, RDE on motorcycles as instruments for future challenges* [online]. [cit. 2020-12-08]. Available at: https://autotechreview.com/cover-stories/pems-rde-on-motorcycles-as-instruments-for-future-challenges

[39] First, Jiří. *Zkoušení automobilů a motocyklů: příručka pro konstruktéry*. Prague: S&T cz, 2008. ISBN 978-80-254-1805-5.

[40] Burtscher, Heinz and W. Majewski. *Exhaust gas sampling and conditioning* [online]. [cit. 2020-12-08]. Available at: https://dieselnet.com/tech/measure_sample.php

[41] Nakamura, Hiroshi and Masayuki Adachi. *Engine emissions measurement handbook: Horiba automotive test systems*. SAE International & Goriba ltd., 2013. ISBN 0768080126.

[42] Martyr, Anthony and M. Plint. *Engine testing: the design, building, modification and use of powertrain test facilities*. 4th edition. Oxford: Butterworth-Heinemann, 2012. ISBN 978-0080969497.

[43] Houghton, E.L. Pitot-static tube. *Science direct* [online]. [cit. 2020-12-08]. Available at: https://www.sciencedirect.com/topics/engineering/pitot-static-tube

[44] Viquerat, Andrew. *A continuous-wave doppler radar system for collision avoidance applications* [online]. [cit. 2020-12-09]. Available at: https://www.researchgate.net/publication/261178925_a_continuous_wave_doppler_radar_system_for_collision_avoidance_applications

[45] *Infrared non-dispersive CO2 analyser working principle* [online]. [cit. 2020-12-08]. Available at: https://instrumentationtools.com/infrared-non-dispersive-co2-analyzer-working-principle/

[46] Clayborne, Andre and Vernon Morris. Fourier transform infrared spectroscopy (FTIR). *Harward University, physical chemistry laboratory* [online]. [cit. 2020-12-08]. Available at: https://chem.libretexts.org/courses/howard_university/howard%3a_physical_chemistry_laboratory/14._fourier_transform_infrared_spectroscopy_(ftir)

[47] Birkner, Nancy et al. *How an FTIR spectrometer operates* [online]. [cit. 2020-12-09]. Available at: https://chem.libretexts.org/bookshelves/physical_and_theoretical_chemistry_textbook_maps/supplemental_modules_(physical_and_theoretical_chemistry)/spectroscopy/vibrational_spectroscopy/infrared_spectroscopy/how_an_ftir_spectrometer_operates

[48] Chemiluminescence. *Servomex* [online]. [cit. 2020-12-08]. Available at: https://www.servomex.com/gas-analyzers/technologies/chemiluminescence/

[49] Hinshaw, John V. The flame ionization detector. *LCQC North America* [online]. [cit. 2020-12-09]. Available at: https://www.chromatographyonline.com/view/flame-ionization-detector

[50] Prasad, Ram. *Catalytic oxidation of diesel soot emission control* [online]. [cit. 2020-12-09]. Available at: https://www.researchgate.net/publication/292138082_catalytic_oxidation_of_diesel_soot_emission_control

[51] *Paramagnetic cells technology for our paramagnetic o2 analyser* [online]. [cit. 2020-12-08]. Available at: https://www.systechillinois.com/en/support/technologies/paramagnetic-cells

[52] Curtis, Dave. Stack emission monitoring: revision to the standard reference methods. *Awe international* [online]. [cit. 2020-12-09]. Available at: https://www.aweimagazine.com/article/stack-emission-monitoring/

[53] Simões Amaral, Simone. An overview of particulate matter measurement instruments. *Atmosphere* [online]. [cit. 2020-12-08]. Available at: https://doi.org/10.3390/atmos6091327

[54] Johnson, T. *An engine exhaust particle sizer spectrometer for transient emission particle measurements* [online]. [cit. 2020-12-09]. Available at: https://www.osti.gov/servlets/purl/829823

[55] Testo NanoMet3 modul for 19“ rack user manual. *Testo SE & CO. KGAA* [online]. [cit. 2020-12-08]. Available at: https://static-int.testo.com/media/70/69/9f79c6aeddeb/testo-nanomet3-instruction-manual.pdf

[56] Document 02018r1832-20181127. *Commission Regulation EU* [online]. [cit. 2020-12-08]. Available at: http://data.europa.eu/eli/reg/2018/1832/2018-11-27

[57] Pohled do zákulisí: jak se měří emise. *Škoda storyboard* [online]. [cit. 2020-12-08]. Available at: https://www.skoda-storyboard.com/cs/skoda-svet-cs/za-oponou-cs/pohled-do-zakulisi-jak-se-meri-emise/

[58] Perujo Mateos Del Parque, Adolfo and Pablo Mendoza Villafuerte. *PEMS emissions testing of heavy duty vehicles/ engines* [online]. [cit. 2020-12-08]. Available at: https://ec.europa.eu/jrc/en/publication/eur-scientific-and-technical-research-reports/pems-emissions-testing-heavy-duty-vehiclesengines-assessment-pems-procedures-fulfilment

[59] *Under the microscope: the PEMS measurement: no two journeys are the same* [online]. [cit. 2020-12-08]. Available at: https://media.daimler.com/marsmediasite/ko/en/42515824

[60] Preda, Ion, Dinu Covaciu and Gheorghe Ciolan. Coast-down test- theoretical and experimental approach. *Transilvania University of Brasov, Romania* [online]. [cit. 2020-12-08]. Available at: http://aspeckt.unitbv.ro/jspui/bitstream/123456789/7/1/conat20104030-paper.pdf

[61] Vojtisek-lom, Michal, Alessandro A. Zardini and Martin Pechout. *A miniature portable emissions measurement system (PEMS) for real-driving monitoring of motorcycles* [online]. [cit. 2020-12-08]. Available at: https://doi.org/10.5194/amt-2019-387

[62] Giechaskiel, Barouch Giechaskiel. Identification and quantification of uncertainty components in gaseous and particle emission measurements of a moped. *Energies* [online]. [cit. 2020-12-08]. Available at: https://www.researchgate.net/publication/337262836_identification_and_quantification_of_uncertainty_components_in_gaseous_and_particle_emission_measurements_of_a_moped

[63] Kontses, A. and B. Giechaskiel. *Particulate emissions from l-category vehicles towards euro 5* [online]. [cit. 2020-12-08]. Available at: https://doi.org/10.1016/j.envres.2019.109071

[64] Císař, Vojtěch. *On-road measurement of exhaust emissions from motorcycles*. Prague, 2020. Diploma thesis. CTU Prague. Thesis supervisor: Vojtíšek M.

[65] *Yamaha XT 660R: review, history, specifications* [online]. [cit. 2020-12-09]. Available at: https://bikeswiki.com/yamaha_xt660r

[66] *Suzuki GSR 600: review, history, specifications* [online]. [cit. 2020-12-09]. Available at: https://bikeswiki.com/suzuki_gsr600

[67] *Mapy.cz* [online]. [cit. 2020-12-11]. Available at: https://mapy.cz/turisticka?mereni-vzdalenosti&x=14.9906402&y=49.4198294&z=15&rm=95fopxug1uhnnmc

List of Tables

Lists of Figures